Electronic Supplementary Information

Highly Asymmetric Lamellar Nanostructures from Nanoparticle–Linear Hybrid Block Copolymers

Kodai Watanabe,[a] Satoshi Katsuhara,[a] Hiroaki Mamiya,[b] Yukihiko Kawamura,[c]

Takuya Yamamoto,[d] Kenji Tajima,[d] Takuya Isono,[*,d] Toshifumi Satoh[*,d]

[a]Graduate School of Chemical Sciences and Engineering, Hokkaido University, Sapporo 060-8628, Japan

[b]Quantum Beam Unit, Advanced Key Technologies Division, National Institute for Materials Science (NIMS), Tsukuba 305-0047, Japan

[c]Neutron Science and Technology Center, Comprehensive Research Organization for Science and Society (CROSS), Tokai 319-1106, Japan

[d]Faculty of Engineering, Hokkaido University, Sapporo 060-8628, Japan

[*]Address correspondence to satoh@eng.hokudai.ac.jp and isono.t@eng.hokudai.ac.jp

Contents

S1. Experimental

1. Materials

sec-Butyllithium (*sec*-BuLi; Kanto Chemical Co., Inc. (Kanto), 1.05 mol L^{-1} in *n*-hexane), *n*-butyllithium (*n*-BuLi; Kanto, 1.01 mol L^{-1} in *n*-hexane), tetrabutylammonium fluoride (TBAF; Tokyo Chemical Industry Co., Ltd. (TCI), 1.0 mol L^{-1} in THF), absolute benzene (Wako Pure Chemical Industries, Ltd., super dehydrated, >99.5%), benzoic acid (TCI, >99.0%), Grubbs 2nd generation catalyst (G2; Sigma-Aldrich Chemicals Co.), and ethyl vinyl ether (TCI, >98.0%) were purchased and used as received. Styrene (S; TCI, >99.0%) and 1,8-diazabicyclo[5.4.0]-7-undecene (DBU; TCI, >98.0%) were purchased and purified by distillation over CaH_2 under vacuum. *rac*-Lactide (LA; TCI, >98.0%) was purchased and purified by recrystallization twice from dry toluene. *p*-3-Butenyl styrene (BS)[1] and (3-bromopropoxy)triisopropylsilane (Br−OTIPS)[2] were prepared according to the reported methods, then further purified by distillation over CaH_2 under vacuum. Commercially available dry THF (Kanto, >99.5%, water content, <0.001%), dry toluene (Kanto, >99.5%, water content, <0.001%), and dry CH_2Cl_2 (Kanto, >99.5%, water content, <0.001%) were further purified by an MBRAUN MB SPS Compact solvent purification system equipped with a MB-KOL-A and a MB-KOL-M Type 1 columns (for dry THF), a MB-KOL-C and a MB-KOL-A columns (for dry toluene), or two MB-KOL-A columns (for dry CH_2Cl_2) which were then directly used for the polymerizations.

2. Instruments

The ring-opening polymerization of *rac*-LA was carried out in an MBRAUN stainless steel glovebox equipped with a gas purification system (molecular sieves and copper catalyst) in a dry argon atmosphere (H_2O, O_2 <1 ppm). The moisture and oxygen contents in the glovebox were monitored by an MB-MO-SE 1 moisture sensor and an MB-OX-SE 1 oxygen sensor, respectively. The ^{1}H (400 MHz) and ^{13}C NMR (100 MHz) spectra were obtained using a JEOL JNM-ESC400 instrument at room temperature. The size exclusion chromatography (SEC) measurements were performed at 40 °C in THF (flow rate, 1.0 mL min^{-1}) using a Jasco high-performance liquid chromatography system (PU-980 Intelligent HPLC Pump, CO-2065 Plus Intelligent Column Oven, RI-2031 Plus Intelligent RI Detector, and DG-2080-53 Degasser) equipped with a Shodex KF-G guard column (4.6 mm × 10 mm; particle size, 8 μm) and two Shodex KF-804L columns (linear; particle size, 7 μm; 8.0 mm × 300 mm; exclusion limit, 4×10^4). Preparative SEC purification was performed in $CHCl_3$ (3.5 mL min^{-1}) at 23 °C using JAI LC-9201 equipped with a JAI JAIGEL-3H column (20 mm × 600 mm; exclusion limit, 7×10^4) and a JAI RI-50s refractive index detector. The Fourier transform infrared spectroscopy (FT-IR) analysis was carried out using a PerkinElmer Frontier MIR spectrometer equipped with a single reflection diamond universal attenuated total reflection (ATR) accessory. Differential scanning calorimetry (DSC) experiments were performed using a Hitachi High-Technologies DSC7000X under a nitrogen atmosphere. All polymers for DSC measurement were heated to 200 °C, cooled to 20 °C, and heated to 200 °C again at the heating and cooling rate of 10 °C min^{-1} and 20 °C min^{-1}, respectively.

3. Synthesis of *ω*-end hydroxy-functionalized statistical copolymer of S and BS ($S_{21}BS_8$−OH).

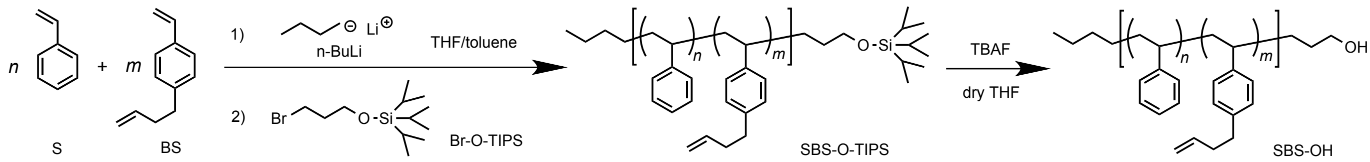

A typical procedure for the synthesis of SBS−OH is as follows (method A). In the glovebox, dry toluene (50 mL) and dry THF (100 mL) were placed in a Schlenk flask. After sealing, the flask was taken out from the glovebox. *sec*-BuLi (100 μL, 105 μmol as a 1.05 mol L^{-1} stock solution in *n*-hexane) was added to the solvent under an Ar atmosphere to remove water completely. Then, the solvent was further purified by trap-to-trap distillation under high vacuum to transfer to another Schlenk flask for polymerization. After cooling to −78 °C, *n*-BuLi (1.97 μmL, 2.39 mmol as a 1.21 mol L^{-1} stock solution in *n*-hexane) was added to the flask. In another flame-dried Schlenk flask, S (5.5 g, 53 mmol) and BS (3.6 g, 23 mmol) were mixed together under an Ar atmosphere. The mixture was added at once to the initiator solution using a syringe. After monomer addition, the mixture was stirred at −78 °C for 6 h. Br−OTIPS (3.57 g, 9.30 mmol) was added to the solution of living polymer anions at −78 °C, and the whole mixture was allowed to react for 1 h at −78 °C and then overnight at room temperature. Afterwards, The solvent was removed from the polymerization mixture under reduced pressure. TBAF (8.35 mL, 8.35 mmol as a 1.0 mol L^{-1} stock solution in THF) and dry THF (20 mL) were added to the crude product at room temperature. After 15 h stirring, the reaction mixture was passed through a short silica-gel column, and the resulting residue was purified by repeated reprecipitation twice from the THF solution into MeOH to give $S_{21}BS_8$−OH as a white solid. Yield: 7.28 g (80%). ^{1}H NMR (400 MHz, $CDCl_3$): δ (ppm) 7.40−6.19 (m, 5H × n + 4H × m, $-C_6H_5$, $-C_6H_4-$), 5.97−5.74 (m, 1H × m, $-CH{=}CH_2$), 5.15−4.90 (m, 2H × m, $-CH{=}CH_2$), 3.47−3.33 (m, 2H, $-CH_2OH$), 2.85−2.45 (m, 2H × m, $-C_6H_4CH_2-$), 2.46−2.14 (m, 2H × m, $-C_6H_4CH_2CH_2-$), 2.15−1.62 (m, 1H × (n+m), $-CH(C_6H_5)-$, $-CH(C_6H_4-)-$), 1.74−0.69 (m, 2H × (m+n) + 9H, $-CH_2CH(C_6H_5)-$, $-CH_2CH(C_6H_4-)-$, C_4H_9-). $M_{n,NMR}$ = 3,600 ($CDCl_3$), the mole fraction of the BS units = 0.29, $M_{n,SEC}$ = 3,920 (THF), $Đ$ = 1.08 (THF).

4. Intramolecular crosslinking of $S_{21}BS_8$−OH via olefin metathesis reaction.

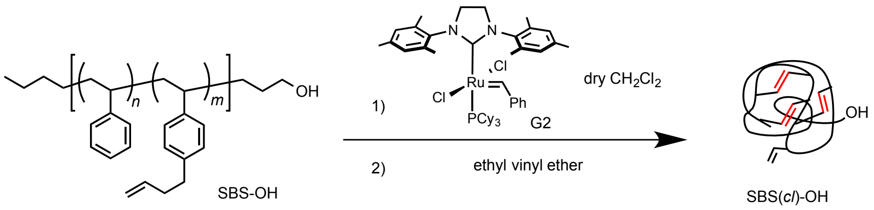

A typical procedure for the intramolecular crosslinking of SBS−OH is as follows (method B). $S_{21}BS_8$−OH ($M_{n,NMR}$ = 3,600, 1.50 g, 3.74 mmol olefin-containing units) was dissolved in dry CH_2Cl_2 (3000 mL). After degassing by N_2 bubbling, G2 (31.7 mg, 37.4 μmol) was added to the mixture. After stirring for 3 h under an N_2 atmosphere at 30 °C, the reaction was quenched by the addition of ethyl vinyl ether. The solvent was removed by evaporation, then the residue was purified by reprecipitation from the CH_2Cl_2 solution into MeOH to give intramolecularly crosslinked $S_{21}BS_8$−OH ($S_{21}BS_8$(*cl*)−OH) as a white solid (1.11 g, 74.0%). The product was further purified by preparative SEC. ^{1}H NMR (400 MHz, $CDCl_3$): δ (ppm) 7.55−5.94 (m, 5H × n + 4H × m, $-C_6H_5$, $-C_6H_4-$), 6.06−4.82 (m, 3H × 0.15m + H × 0.85m, $-CH{=}CH_2$, $-CH{=}CH-$, $-CH{=}CH_2$), 3.62−3.23 (m, 2H, $-CH_2OH$), 3.14−0.64 (m, 7H × m + 3H × n + 9H, $-C_6H_4CH_2-$, $-C_6H_4CH_2CH_2-$, $-CH(C_6H_5)-$, $-CH(C_6H_4-)-$, $-CH_2CH(C_6H_5)-$, $-CH_2CH(C_6H_4-)-$, C_4H_9-). $M_{n,SEC}$ = 2,790 (THF), $Đ$ = 1.18 (THF), the conversion of the terminal olefins = 85%.

5. Synthesis of block copolymer consisting of SBS(*cl*) and poly(*rac*-LA) ($S_{21}BS_8$(*cl*)−LA_{20}) via ring-opening polymerization of *rac*-LA using $S_{21}BS_8$(*cl*)−OH as an initiator.

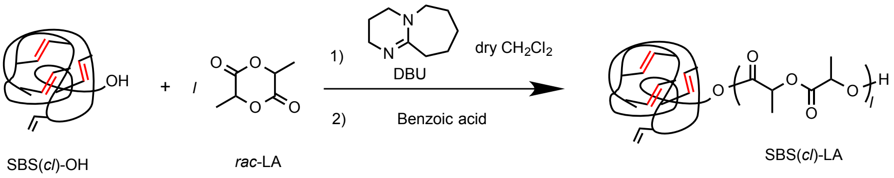

A typical procedure for the polymerization of *rac*-LA is as follows (method C). $S_{21}BS_8$(*cl*)−OH was freeze-dried from its absolute benzene solution three times prior to the polymerization. In the glovebox, $S_{21}BS_8$(*cl*)−OH ($M_{n,NMR}$ = 3,500, 234 mg, 66.9 μmol) and *rac*-LA (293 mg, 2.03 mmol) were dissolved in dry CH_2Cl_2 (4.10 mL). DBU (3.0 μL, 20.3 μmol) was then added to the CH_2Cl_2 solution to initiate the polymerization. After 8 min, the polymerization was quenched by the addition of benzoic acid. The mixture was purified by reprecipitation from the CH_2Cl_2 solution into MeOH to give $S_{21}BS_8$(*cl*)−LA_{20} as a white solid (394 mg, 81.1%). The product was further purified by preparative SEC. ^{1}H NMR (400 MHz, $CDCl_3$): δ (ppm) 7.55−5.94 (m, 5H × n + 4H × m, $-C_6H_5$, $-C_6H_4-$), 6.06−4.82 (m, 3H × 0.15m + H × 0.85m + 1H × (2l-1), $-CH{=}CH_2$, $-CH{=}CH-$, $-CH{=}CH_2$, $-OCOCH(CH_3)-$), 4.43−4.28 (m, 1H, $-CH(CH_3)OH$), 4.07−3.78 (m, 2H, $-C_2H_4CH_2OCO-$), 3.14−0.64 (m, 7H × m + 3H × n + 3H × 2l + 9H, $-C_6H_4CH_2-$, $-C_6H_4CH_2CH_2-$, $-CH(C_6H_5)-$, $-CH(C_6H_4-)-$, $-CH_2CH(C_6H_5)-$, $-CH_2CH(C_6H_4-)-$, $-OCOCH(CH_3)-$, C_4H_9-). Conversion = 86%, $M_{n,NMR}$ = 6,430 ($CDCl_3$), the weight fraction of PLA = 0.46, $M_{n,SEC}$ = 14,900 (THF), $Đ$ = 1.06 (THF).

Synthesis of ω-end hydroxy-functionalized statistical copolymer of S and BS ($S_{33}BS_{14}$–OH). Method A was used for the living anionic copolymerization of S (5.5 g, 53 mmol) and BS (3.6 g, 23 mmol) with *n*-BuLi (1.21 mL, 1.61 mmol as a 1.33 mol L^{-1} stock solution in *n*-hexane) and Br–O–TIPS (1.53 g, 5.17 mmol) in mixture solvent of dry toluene (100 mL) and dry THF (50 mL) for 6 h followed by the deprotection with TBAF (15.5 mL, 15.5 mmol as a 1.0 mol L^{-1} stock solution in THF) in dry THF (50 mL) to give $S_{33}BS_{14}$–OH. Yield: 8.02 g (88 %). $M_{n,NMR}$ = 5,760 ($CDCl_3$), f_{BS} = 0.30, $M_{n,SEC}$ = 6,070 (THF), $Đ$ = 1.04 (THF).

Synthesis of ω-end hydroxy-functionalized statistical copolymer of S and BS ($S_{65}BS_{28}$–OH). Method A was used for the living anionic copolymerization of S (5.5 g, 53 mmol) and BS (3.6 g, 23 mmol) with *n*-BuLi (0.92 mL, 0.82 mmol as a 0.89 mol L^{-1} stock solution in *n*-hexane) and Br–O–TIPS (1.41 g, 4.79 mmol) in mixture solvent of dry toluene (100 mL) and dry THF (50 mL) for 6 h followed by the deprotection with TBAF (14.4 mL, 14.4 mmol as a 1.0 mol L^{-1} stock solution in THF) in dry THF (50 mL) to give $S_{65}BS_{28}$–OH. Yield: 8.02 g (88 %). $M_{n,NMR}$ = 11,100 ($CDCl_3$), f_{BS} = 0.30, $M_{n,SEC}$ = 11,200 (THF), $Đ$ = 1.04 (THF).

Synthesis of ω-end hydroxy-functionalized statistical copolymer of S and BS ($S_{47}BS_{47}$–OH). Method A was used for the living anionic copolymerization of S (3.9 g, 38 mmol) and BS (5.9 g, 38 mmol) with *n*-BuLi (0.92 mL, 0.80 mmol as a 0.87 mol L^{-1} stock solution in *n*-hexane) and Br–O–TIPS (1.99 g, 6.37 mmol) in mixture solvent of dry toluene (100 mL) and dry THF (50 mL) for 6 h followed by the deprotection with TBAF (20.2 mL, 20.2 mmol as a 1.0 mol L^{-1} stock solution in THF) in dry THF (50 mL) to give $S_{47}BS_{47}$–OH. Yield: 8.69 g (89 %). $M_{n,NMR}$ = 12,400 ($CDCl_3$), f_{BS} = 0.50, $M_{n,SEC}$ = 12,200 (THF), $Đ$ = 1.06 (THF).

Intramolecular crosslinking of $S_{33}BS_{14}$–OH via olefin metathesis reaction. Method B was used for the intramolecular crosslinking of $S_{33}BS_{14}$–OH ($M_{n,NMR}$ = 5,760, 1.50 g, 3.74 mmol olefin-containing units) with G2 (31.7 mg, 37.4 μmol) in dry CH_2Cl_2 (3000 mL) for 3 h to give

$S_{33}BS_{14}$(*cl*)–OH as a white solid (1.20 g, 80.0 %)). The product was further purified by preparative SEC prior to each measurement. $M_{n,SEC}$ = 4,880 (THF), $Đ$ = 1.09 (THF), conv.$_{olefin}$ = 86%.

Intramolecular crosslinking of $S_{65}BS_{28}$–OH via olefin metathesis reaction. Method B was used for the intramolecular crosslinking of $S_{65}BS_{28}$–OH ($M_{n,NMR}$ = 11,100, 1.00 g, 2.49 mmol olefin-containing units) with G2 (21.2 mg, 24.9 μmol) in dry CH_2Cl_2 (3330 mL) for 3 h to give $S_{65}BS_{28}$(*cl*)–OH as a white solid (740 mg, 74.0 %)). The product was further purified by preparative SEC prior to each measurement. $M_{n,SEC}$ = 7,870 (THF), $Đ$ = 1.06 (THF), conv.$_{olefin}$ = 88%.

Intramolecular crosslinking of $S_{47}BS_{47}$–OH via olefin metathesis reaction. Method B was used for the intramolecular crosslinking of $S_{47}BS_{47}$–OH ($M_{n,NMR}$ = 12,400, 1.00 g, 3.81 mmol olefin-containing units) with G2 (32.4 mg, 38.1 μmol) in dry CH_2Cl_2 (3330 mL) for 3 h to give $S_{65}BS_{28}$(*cl*)–OH as a white solid (830 mg, 83.0 %)). The product was further purified by preparative SEC prior to each measurement. $M_{n,SEC}$ = 7,120 (THF), $Đ$ = 1.04 (THF), conv.$_{olefin}$ = 84%.

Synthesis of block copolymer consisting of SBS(*cl*) and poly(*rac*-LA) ($S_{21}BS_8$(*cl*)–LA_{45}) via ring-opening polymerization of *rac*-LA using $S_{21}BS_8$(*cl*)–OH as an initiator. Method C was used for the ring-opening polymerization of *rac*-LA (375 mg, 2.60 mmol) with $S_{21}BS_8$(*cl*)–OH ($M_{n,NMR}$ = 3,500, 150 mg, 42.9 μmol) and DBU (3.9 μL, 26 μmol) in dry CH_2Cl_2 (5.2 mL) for 15 min to give $S_{21}BS_8$(*cl*)–LA_{45} as a white solid (409 mg, 77.9%)). The product was further purified by preparative SEC prior to the intramolecular crosslinking reaction and each measurement. $M_{n,NMR}$ = 10,100 ($CDCl_3$), F_{LA} = 0.65, $M_{n,SEC}$ = 15,500 (THF), $Đ$ = 1.04 (THF).

Synthesis of block copolymer consisting of SBS(*cl*) and poly(*rac*-LA) ($S_{21}BS_8$(*cl*)–LA_{70}) via ring-opening polymerization of *rac*-LA using $S_{21}BS_8$(*cl*)–OH as an initiator. Method C was used for the ring-opening polymerization of *rac*-LA (488 mg, 3.38 mmol) with $S_{21}BS_8$(*cl*)–OH ($M_{n,NMR}$ = 3,500, 130 mg, 37.1 μmol) and DBU (5.1 μL, 34 μmol) in dry CH_2Cl_2 (6.8 mL) for 25 min to give $S_{21}BS_8$(*cl*)–LA_{70} as a white solid (469 mg, 75.9%)). The product was further purified by preparative SEC prior to the intramolecular crosslinking reaction and each measurement. Conversion = 85%, $M_{n,NMR}$ = 20,900 ($CDCl_3$), F_{LA} = 0.65, $M_{n,SEC}$ = 11,700 (THF), $Đ$ = 1.05 (THF).

Synthesis of block copolymer consisting of SBS(*cl*) and poly(*rac*-LA) ($S_{21}BS_8$(*cl*)−LA_{110}) via ring-opening polymerization of *rac*-LA using $S_{21}BS_8$(*cl*)−OH as an initiator. Method C was used for the ring-opening polymerization of *rac*-LA (531 mg, 3.69 mmol) with $S_{21}BS_8$(*cl*)–OH ($M_{n,NMR}$ = 3,500, 85 mg, 24.3 μmol) and DBU (5.5 μL, 37 μmol) in dry CH_2Cl_2 (7.4 mL) for 35 min to give $S_{21}BS_8$(*cl*)–LA_{70} as a white solid (407 mg, 66.1%)). The product was further purified by preparative SEC prior to the intramolecular crosslinking reaction and each measurement. Conversion = 76%, $M_{n,NMR}$ = 19,400 ($CDCl_3$), F_{LA} = 0.82, $M_{n,SEC}$ = 25,200 (THF), $Đ$ = 1.03 (THF).

Synthesis of block copolymer consisting of SBS(*cl*) and poly(*rac*-LA) ($S_{33}BS_{14}$(*cl*)−LA_{33}) via ring-opening polymerization of *rac*-LA using $S_{33}BS_{14}$(*cl*)−OH as an initiator. Method C was used for the ring-opening polymerization of *rac*-LA (293 mg, 2.03 mmol) with $S_{33}BS_{14}$(*cl*)–OH ($M_{n,NMR}$ = 5,600, 234 mg, 41.8 μmol) and DBU (3.0 μL, 20 μmol) in dry CH_2Cl_2 (4.1 mL) for 12 min to give $S_{33}BS_{14}$(*cl*)–LA_{33} as a white solid (386 mg, 73.2%)). The product was further purified by preparative SEC prior to the intramolecular crosslinking reaction and each measurement. Conversion = 85%, $M_{n,NMR}$ = 10,400 ($CDCl_3$), F_{LA} = 0.46, $M_{n,SEC}$ = 14,900 (THF), $Đ$ = 1.06 (THF).

Synthesis of block copolymer consisting of SBS(*cl*) and poly(*rac*-LA) ($S_{33}BS_{14}$(*cl*)−LA_{72}) via ring-opening polymerization of *rac*-LA using $S_{33}BS_{14}$(*cl*)−OH as an initiator. Method C was used for the ring-opening polymerization of *rac*-LA (375 mg, 2.60 mmol) with $S_{33}BS_{14}$(*cl*)–OH ($M_{n,NMR}$ = 5,600, 150 mg, 26.8 μmol) and DBU (3.9 μL, 26 μmol) in dry CH_2Cl_2 (5.2 mL) for 23 min to give $S_{33}BS_{14}$(*cl*)–LA_{72} as a white solid (415 mg, 79.0%)). The product was further purified by preparative SEC prior to the intramolecular crosslinking reaction and each measurement. Conversion = 79%, $M_{n,NMR}$ = 16,000 ($CDCl_3$), F_{LA} = 0.65, $M_{n,SEC}$ = 23,200 (THF), $Đ$ = 1.07 (THF).

Synthesis of block copolymer consisting of SBS(*cl*) and poly(*rac*-LA) ($S_{33}BS_{14}$(*cl*)−LA_{112})

via ring-opening polymerization of *rac*-LA using $S_{33}BS_{14}$(*cl*)−OH as an initiator. Method C was used for the ring-opening polymerization of *rac*-LA (479 mg, 3.32 mmol) with $S_{33}BS_{14}$(*cl*)–OH ($M_{n,NMR}$ = 5,600, 130 mg, 23.2 μmol) and DBU (5.0 μL, 33 μmol) in dry CH_2Cl_2 (6.6 mL) for 35 min to give $S_{33}BS_{14}$(*cl*)–LA_{112} as a white solid (446 mg, 73.2%)). The product was further purified by preparative SEC prior to the intramolecular crosslinking reaction and each measurement. Conversion = 82%, $M_{n,NMR}$ = 21,800 ($CDCl_3$), F_{LA} = 0.74, $M_{n,SEC}$ = 29,800 (THF), $Đ$ = 1.05 (THF).

Synthesis of block copolymer consisting of SBS(*cl*) and poly(*rac*-LA) ($S_{33}BS_{14}$(*cl*)−LA_{201}) via ring-opening polymerization of *rac*-LA using $S_{33}BS_{14}$(*cl*)−OH as an initiator. Method C was used for the ring-opening polymerization of *rac*-LA (531 mg, 3.69 mmol) with $S_{33}BS_{14}$(*cl*)–OH ($M_{n,NMR}$ = 5,600, 85.0 mg, 24.3 μmol) and DBU (5.5 μL, 37 μmol) in dry CH_2Cl_2 (7.4 mL) for 55 min to give $S_{33}BS_{14}$(*cl*)–LA_{201} as a white solid (451 mg, 73.2%)). The product was further purified by preparative SEC prior to the intramolecular crosslinking reaction and each measurement. Conversion = 88%, $M_{n,NMR}$ = 34,500 ($CDCl_3$), F_{LA} = 0.82, $M_{n,SEC}$ = 39,900 (THF), $Đ$ = 1.06 (THF).

Synthesis of block copolymer consisting of SBS(*cl*) and poly(*rac*-LA) ($S_{65}BS_{28}$(*cl*)−LA_{74}) via ring-opening polymerization of *rac*-LA using $S_{65}BS_{28}$(*cl*)−OH as an initiator. Method C was used for the ring-opening polymerization of *rac*-LA (143 mg, 990 μmol) with $S_{65}BS_{28}$(*cl*)–OH ($M_{n,NMR}$ = 10,800, 100 mg, 9.35 μmol) and DBU (1.5 μL, 10 μmol) in dry CH_2Cl_2 (2.0 mL) for 20 min to give $S_{65}BS_{28}$(*cl*)–LA_{74} as a white solid (181 mg, 74.5%)). The product was further purified by preparative SEC prior to the intramolecular crosslinking reaction and each measurement. Conversion = 68%, $M_{n,NMR}$ = 21,500 ($CDCl_3$), F_{LA} = 0.50, $M_{n,SEC}$ = 18,800 (THF), $Đ$ = 1.09 (THF).

Synthesis of block copolymer consisting of SBS(*cl*) and poly(*rac*-LA) ($S_{65}BS_{28}$(*cl*)−LA_{160}) via ring-opening polymerization of *rac*-LA using $S_{65}BS_{28}$(*cl*)−OH as an initiator. Method C was used for the ring-opening polymerization of *rac*-LA (185 mg, 1.28 mmol) with $S_{65}BS_{28}$(*cl*)–OH ($M_{n,NMR}$ = 10,800, 65.0 mg, 6.07 μmol) and DBU (1.9 μL, 13 μmol) in dry CH_2Cl_2 (2.6 mL) for 45 min to give

$S_{65}BS_{28}(cl)–LA_{160}$ as a white solid (184 mg, 73.6%)). The product was further purified by preparative SEC prior to the intramolecular crosslinking reaction and each measurement. Conversion = 74%, $M_{n,NMR}$ = 33,800 ($CDCl_3$), F_{LA} = 0.68, $M_{n,SEC}$ = 32,100 (THF), $Đ$ = 1.06 (THF).

Synthesis of block copolymer consisting of SBS(*cl*) and poly(*rac*-LA) ($S_{65}BS_{28}(cl)–LA_{223}$) via ring-opening polymerization of *rac*-LA using $S_{65}BS_{28}(cl)–OH$ as an initiator. Method C was used for the ring-opening polymerization of *rac*-LA (213 mg, 1.48 mmol) with $S_{65}BS_{28}(cl)–OH$ ($M_{n,NMR}$ = 10,800, 50.0 mg, 4.67 μmol) and DBU (2.2 μL, 15 μmol) in dry CH_2Cl_2 (3.0 mL) for 65 min to give $S_{65}BS_{28}(cl)–LA_{223}$ as a white solid (185 mg, 93%)). The product was further purified by preparative SEC prior to the intramolecular crosslinking reaction and each measurement. Conversion = 78%, $M_{n,NMR}$ = 42,900 ($CDCl_3$), F_{LA} = 0.75, $M_{n,SEC}$ = 40,700 (THF), $Đ$ = 1.06 (THF).

Synthesis of block copolymer consisting of SBS(*cl*) and poly(*rac*-LA) ($S_{65}BS_{28}(cl)–LA_{459}$) via ring-opening polymerization of *rac*-LA using $S_{65}BS_{28}(cl)–OH$ as an initiator. Method C was used for the ring-opening polymerization of *rac*-LA (249 mg, 1.72 mmol) with $S_{65}BS_{28}(cl)–OH$ ($M_{n,NMR}$ = 10,800, 35.0 mg, 3.27 μmol) and DBU (2.6 μL, 17 μmol) in dry CH_2Cl_2 (3.4 mL) for 90 min to give $S_{65}BS_{28}(cl)–LA_{459}$ as a white solid (232 mg, 81.4%)). The product was further purified by preparative SEC prior to the intramolecular crosslinking reaction and each measurement. Conversion = 83%, $M_{n,NMR}$ = 76,900 ($CDCl_3$), F_{LA} = 0.86, $M_{n,SEC}$ = 56,000 (THF), $Đ$ = 1.09 (THF).

Synthesis of block copolymer consisting of SBS(*cl*) and poly(*rac*-LA) ($S_{65}BS_{28}(cl)–LA_{684}$) via ring-opening polymerization of *rac*-LA using $S_{65}BS_{28}(cl)–OH$ as an initiator. Method C was used for the ring-opening polymerization of *rac*-LA (249 mg, 1.72 mmol) with $S_{65}BS_{28}(cl)–OH$ ($M_{n,NMR}$ = 10,800, 25.0 mg, 2.34 μmol) and DBU (2.6 μL, 17 μmol) in dry CH_2Cl_2 (3.4 mL) for 110 min to give $S_{65}BS_{28}(cl)–LA_{684}$ as a white solid (236 mg, 86.2%)). Conversion = 92%, $M_{n,NMR}$ = 109,000 ($CDCl_3$), F_{LA} = 0.90, $M_{n,SEC}$ = 60,600 (THF), $Đ$ = 1.14 (THF).

Synthesis of block copolymer consisting of SBS(*cl*) and poly(*rac*-LA) ($S_{65}BS_{28}(cl)–LA_{923}$)

via ring-opening polymerization of *rac*-LA using $S_{65}BS_{28}$(*cl*)−OH as an initiator. Method C was used for the ring-opening polymerization of *rac*-LA (257 mg, 1.78 mmol) with $S_{65}BS_{28}$(*cl*)–OH ($M_{n,NMR}$ = 10,800, 18 mg, 1.68 μmol) and DBU (2.7 μL, 18 μmol) in dry CH_2Cl_2 (3.6 mL) for 140 min to give $S_{65}BS_{28}$(*cl*)–LA_{923} as a white solid (226 mg, 82.1%)). The product was further purified by preparative SEC prior to the intramolecular crosslinking reaction and each measurement. Conversion = 82%, $M_{n,NMR}$ = 144,000 ($CDCl_3$), F_{LA} = 0.92, $M_{n,SEC}$ = 60,200 (THF), $Đ$ = 1.10 (THF).

Synthesis of block copolymer consisting of SBS(*cl*) and poly(*rac*-LA) ($S_{47}BS_{47}$(*cl*)−LA_{484}) via ring-opening polymerization of *rac*-LA using $S_{47}BS_{47}$(*cl*)−OH as an initiator. Method C was used for the ring-opening polymerization of *rac*-LA (129 mg, 0.89 mmol) with $S_{47}BS_{47}$(*cl*)–OH ($M_{n,NMR}$ = 11,800, 20 mg, 1.69 μmol) and DBU (1.3 μL, 8.9 μmol) in dry CH_2Cl_2 (1.8 mL) for 90 min to give $S_{47}BS_{47}$(*cl*)–LA_{484} as a white solid (99.0 mg, 66.4%)). The product was further purified by preparative SEC prior to the intramolecular crosslinking reaction and each measurement. Conversion = 91%, $M_{n,NMR}$ = 81,600 ($CDCl_3$), F_{LA} = 0.86, $M_{n,SEC}$ = 55,900 (THF), $Đ$ = 1.07 (THF).

Synthesis of block copolymer consisting of SBS and poly(*rac*-LA) ($S_{65}BS_{28}$−LA_{67}) via ring-opening polymerization of *rac*-LA using $S_{65}BS_{28}$−OH as an initiator. Method C was used for the ring-opening polymerization of *rac*-LA (163 mg, 1.13 mmol) with $S_{65}BS_{28}$–OH ($M_{n,NMR}$ = 11,100, 100 mg, 9.01 μmol) and DBU (1.7 μL, 11.3 μmol) in dry CH_2Cl_2 (4.5 mL) for 90 min to give $S_{65}BS_{28}$–LA_{67} as a white solid (214.3 mg, 81.5%)). Conversion = 70%, $M_{n,NMR}$ = 20,800 ($CDCl_3$), F_{LA} = 0.47, $M_{n,SEC}$ = 24,000 (THF), $Đ$ = 1.05 (THF).

Synthesis of block copolymer consisting of SBS and poly(*rac*-LA) ($S_{65}BS_{28}$−LA_{466}) via ring-opening polymerization of *rac*-LA using $S_{65}BS_{28}$−OH as an initiator. Method C was used for the ring-opening polymerization of *rac*-LA (445 mg, 3.09 mmol) with $S_{65}BS_{28}$–OH ($M_{n,NMR}$ = 11,100, 60.0 mg, 5.41 μmol) and DBU (4.6 μL, 30.9 μmol) in dry CH_2Cl_2 (6.2 mL) for 100 min to give $S_{65}BS_{28}$–LA_{466} as a white solid (430.1 mg, 85.3%)). Conversion = 82%, $M_{n,NMR}$ = 77,600 ($CDCl_3$), F_{LA} = 0.86, $M_{n,SEC}$ =

62,700 (THF), $Đ$ = 1.09 (THF).

6. Small-angle X-ray Scattering (SAXS)

The morphologies and *d*-values of samples in the bulk state were investigated using SAXS. Experiments were performed on the BL-6A beamline at the Photon Factory in the High Energy Accelerator Research Organization (KEK, Tsukuba, Japan) using X-ray beams with λ = 1.5 Å. 2D scattering patterns were collected with a PILATUS3 1M detector (Dectris Ltd.), where the sample-to-detector distance was set to 1.5 m. The scattering angle (θ) was calibrated using silver behenate (Nagara Science Co., Ltd.) as the standard and subsequently converted to the scattering vector (q) using Bragg's equation ($q = (4\pi/\lambda)\sin(\theta/2)$). The *d*-values of the samples were calculated according to $d = 2\pi/q^*$, where q^* is the principal scattering peak position. The bulk samples obtained after reprecipitation and vacuum drying were annealed at an appropriate temperature (150 °C for $S_{21}BS_8(cl)$–LAs, $S_{33}BS_{14}(cl)$–LAs, and $S_{65}BS_{28}(cl)$–LAs; 180 °C for $S_{47}BS_{47}(cl)$–LA_{484}; 130 °C for $S_{65}BS_{28}$–LA_{67} and $S_{65}BS_{28}$–LA_{466}) for 1 h under vacuum, and then directly exposed to X-rays for 1 min each.

7. Grazing Incidence SAXS (GISAXS)

The morphologies and *d*-values of the samples in the thin film state were investigated using GISAXS. Experiments were performed on the BL-6A beamline of KEK using X-ray beams with λ = 1.5 Å. The sample-to-detector distance was set to 2.0 m. The 2D GISAXS profiles were acquired under ambient conditions for 20 s at various incidence angles. Prior to the thin film preparation, polystyrene-*random*-poly(methyl methacrylate) with ~ 20 mol% polystyrene ($PS_{0.2}$-*r*-$PMMA_{0.8}$) were grafted on to a Si substrate to generate a brush underlayer. The thin films for GISAXS experiments were prepared via spin-coating (2000 rpm for 1 min) the polymer solution in toluene (0.66 wt%) onto the chemically modified Si substrate. The obtained thin film samples were annealed at 180 °C for 30 min.

The film thickness was measured by ellipsometry (JASCO M-500S).

8. Transmission Electron Microscopy (TEM)

Bright-field TEM images of the thinly sliced bulk samples were obtained using a JEM-3200FS electron microscope (JEOL) with an accelerating voltage of 100 kV. Bulk film samples were prepared by drop-casting from the toluene solutions followed by annealing at 150 °C ($S_{65}BS_{28}(cl)$–LA_{74}) or 180 °C ($S_{47}BS_{47}(cl)$–LA_{484}) for 1 h under vacuum, and then embedding in a photocurable resin (Toagosei Co., Ltd., Alonix D-800). Sample slices with a thickness of ~ 40 nm were obtained using a Leica Ultracut S ultramicrotome equipped with a diamond knife (DiATOME, ultra sonic) at 25 °C, and a piece of each slice was transferred to a copper grid. Subsequently, the $S_{65}BS_{28}(cl)$–LA_{74} sample on the grid was stained by exposure to the vapor of a 0.5% aqueous RuO_4 solution for 10 h.

9. Small-Angle Neutron Scattering (SANS)

The R_g of samples in the bulk state were determined by SANS analysis. The experiments were performed using a time-of-flight small and wide angle neutron scattering instrument (TAIKAN) installed on the BL15 beamline at the Material and Life Science Experimental Facility (MLF) in the Japan Proton Accelerator Research Complex (J-PARC, Tokai, Japan) using white neutron beams in the λ range of 0.7-7.8 Å. The scattering patterns were collected with 1608 ^3He 1D position-sensitive detectors (Canon Electron Tubes & Devices Co., Ltd.) in a small-angle detector bank located at about 5.6 m away from the sample position.[3] Data processing was performed using a software UTSUSEMI. Binary blend samples composed of the deuterated polystyrene with DP of ~ 80 (d-PS_{80}; M_n = 8,800, $Đ$ = 1.02, Polymer Source, Inc.) and hydrogenous samples ($S_{65}BS_{28}$–OH or $S_{65}BS_{28}(cl)$–OH) were prepared as follows. The powdered mixture of d-PS_{80} (188 mg) and hydrogenous polystyrene (172 mg) was dissolved in toluene (500 μL) and vortexed for 1 h. The solution was then cast into a 15 mm diameter mold made from aluminum foil and dried at 25 °C for 24 h, then at 60 °C for 15 h, and finally at 130 °C for 5 h to completely remove the residual solvent. The dried sample was then annealed at 130 °C for 2 h under vacuum to yield the polymer discs with a thickness of ~ 2 mm. The obtained discs were directly exposed to the neutron beam for 30 min each without peeling the aluminum foil off.

10. Atomic Force Microscopy (AFM)

The AFM phase images were obtained using a Molecular Imaging PicoPlus atomic force microscope operating in the tapping mode with a silicon cantilever having a resonant frequency of 190 kHz and a force constant of 48 N m^{-1} (Nanoworld AG, NANOSENSORS^{TM} PPP-NCH). The thin film samples were the same as those used for the GISAXS experiments.

S2. Figures and Table Cited in Main Text

Table S1. Characterization data of SBS–OHs and SBS(*cl*)–OHs

sample name	$f_{\mathrm{BS}}{}^{a}$	conv.$_{\mathrm{olefin}}{}^{a}$ (%)	$M_{\mathrm{n,NMR}}{}^{a}$	$M_{\mathrm{n,SEC}}{}^{b}$	$Đ^{b}$	$T_{\mathrm{g}}{}^{c}$ (°C)	$R_{\mathrm{g}}{}^{d}$ (nm)
$S_{21}BS_8$–OH	0.29	–	3,600	3,920	1.08	53.2	–
$S_{21}BS_8$(*cl*)–OH	–	85	3,500	2,790	1.18	104.4	–
$S_{33}BS_{14}$–OH	0.30	–	5,760	6,070	1.04	62.3	–
$S_{33}BS_{14}$(*cl*)–OH	–	86	5,600	4,880	1.09	125.7	–
$S_{65}BS_{28}$–OH	0.30	–	11,100	11,200	1.04	68.8	2.9
$S_{65}BS_{28}$(*cl*)–OH	–	88	10,800	7,870	1.06	137.1	2.5
$S_{47}BS_{47}$–OH	0.50	–	12,400	12,200	1.06	54.5	2.9
$S_{47}BS_{47}$(*cl*)–OH	–	84	11,800	7,120	1.04	148.1	2.2

[a]Determined by ^{1}H NMR in $CDCl_3$. [b]Determined by SEC in THF using polystyrene standards. [c]Determined by DSC at the heating rate of 10 °C min^{-1}. [d]Determined by SANS in the bulk.

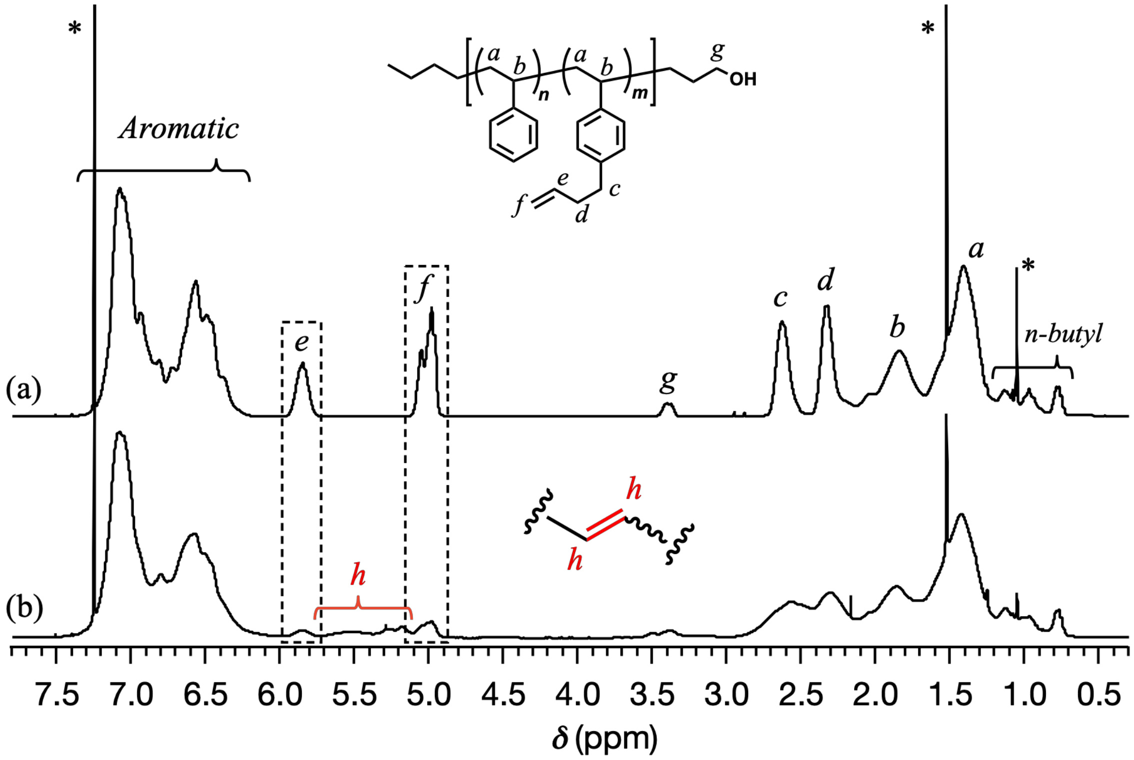

Figure S1. ^{1}H NMR spectra of (a) $S_{21}BS_8$–OH and (b) $S_{21}BS_8$(*cl*)–OH in $CDCl_3$ (400 MHz).

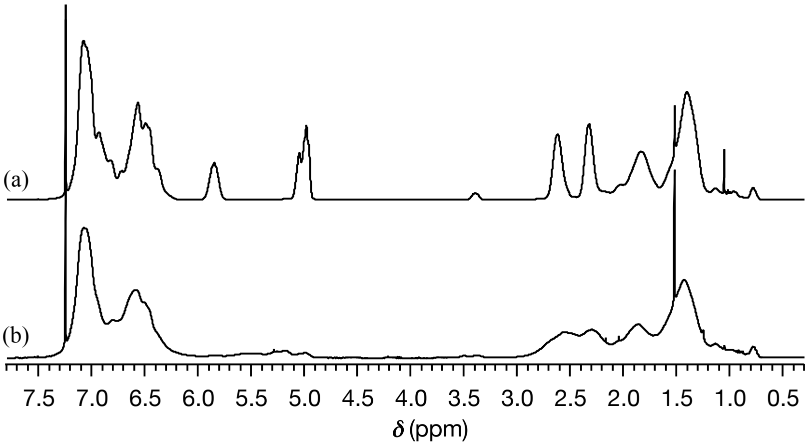

Figure S2. ^{1}H NMR spectra of (a) $S_{33}BS_{14}$–OH and (b) $S_{33}BS_{14}$(*cl*)–OH in $CDCl_3$ (400 MHz).

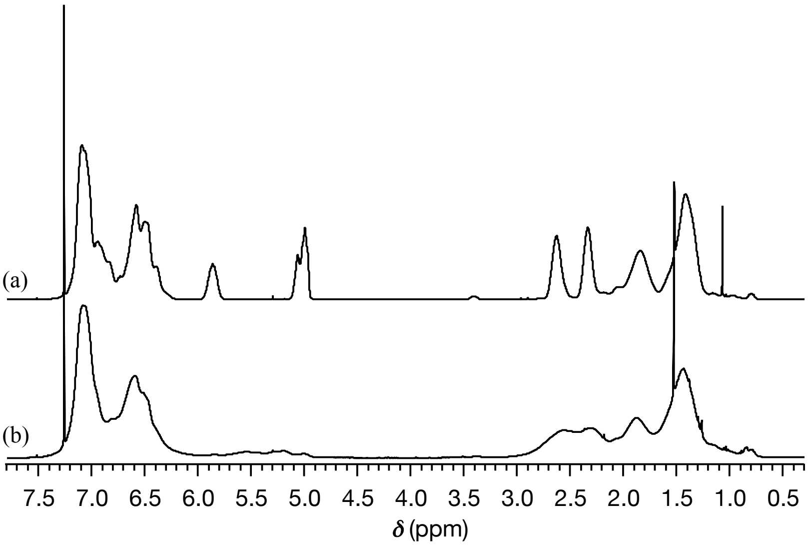

Figure S3. ^{1}H NMR spectra of (a) $S_{65}BS_{28}$–OH and (b) $S_{65}BS_{28}$(*cl*)–OH in $CDCl_3$ (400 MHz).

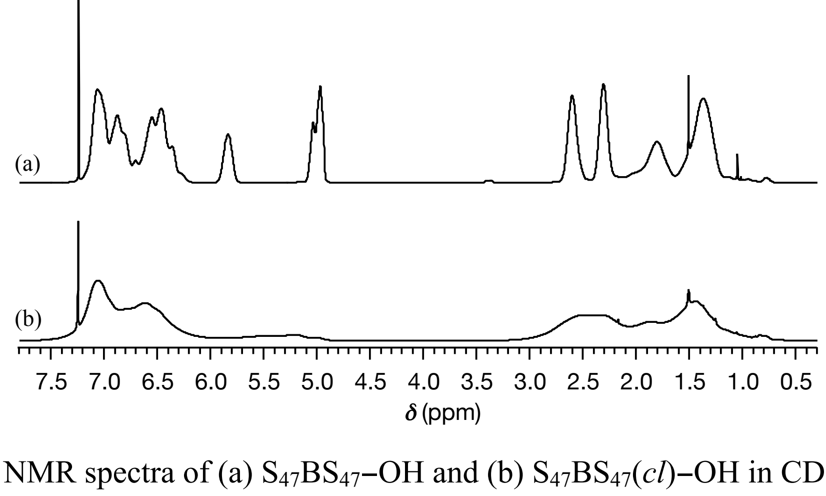

Figure S4. ^{1}H NMR spectra of (a) $S_{47}BS_{47}$–OH and (b) $S_{47}BS_{47}$(*cl*)–OH in $CDCl_3$ (400 MHz).

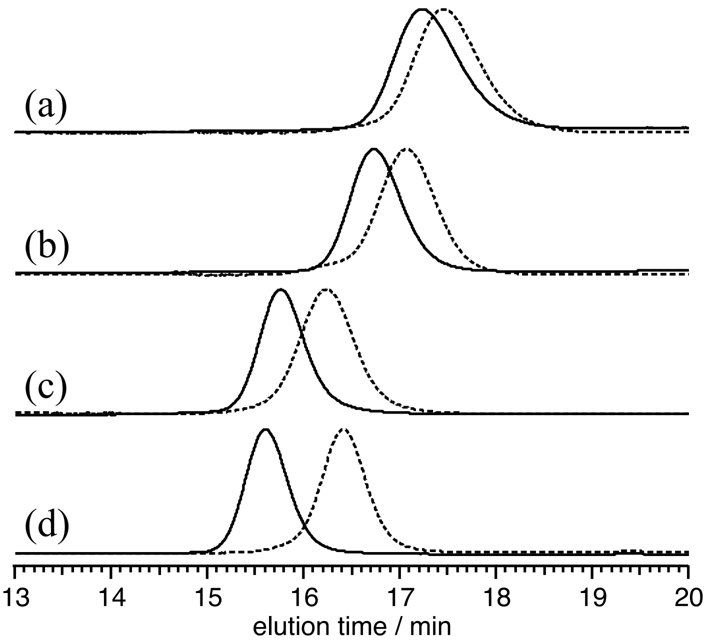

Figure S5. SEC traces of (a) $S_{21}B_8$–OH and $S_{21}BS_8$(*cl*)–OH, (b) $S_{33}BS_{14}$–OH and $S_{33}BS_{14}$(*cl*)–OH, (c) $S_{65}BS_{28}$–OH and $S_{65}BS_{28}$(*cl*)–OH, and (d) $S_{47}BS_{47}$–OH and $S_{47}BS_{47}$(*cl*)–OH (eluent, THF; flow rate, 1.0 mL min^{-1}). SBS–OHs and SBS(*cl*)–OHs are presented using solid and dashed lines, respectively.

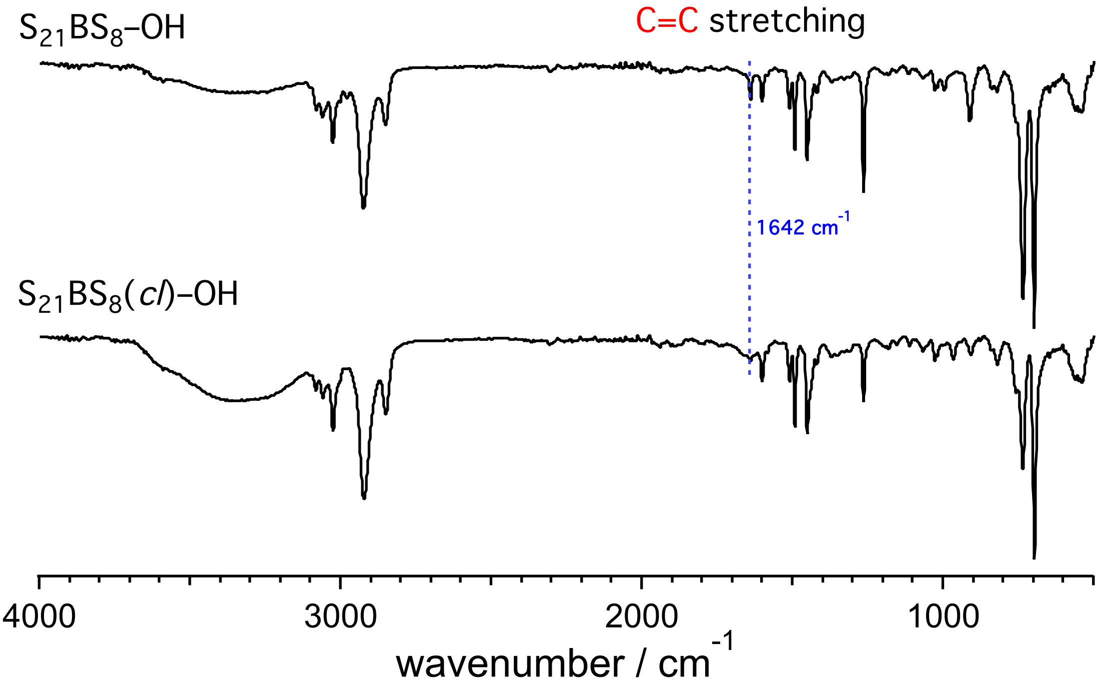

Figure S6. IR spectra of $S_{21}BS_8$–OH (upper) and $S_{21}BS_8$(*cl*)–OH (lower).

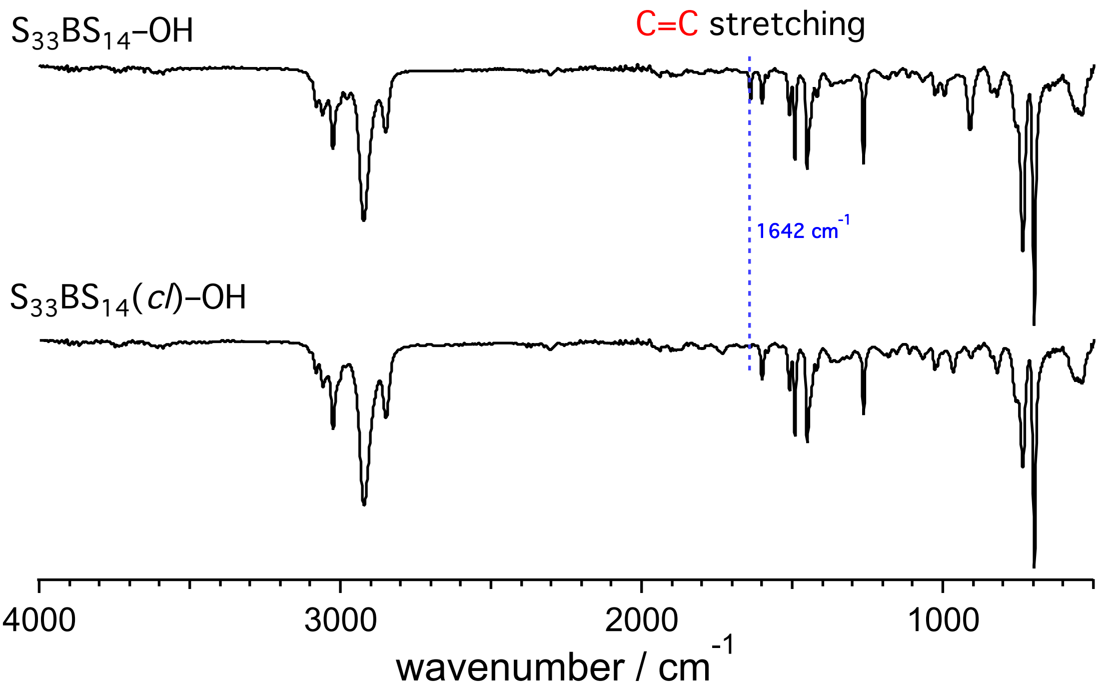

Figure S7. IR spectra of $S_{33}BS_{14}$–OH (upper) and $S_{33}BS_{14}$(*cl*)–OH (lower).

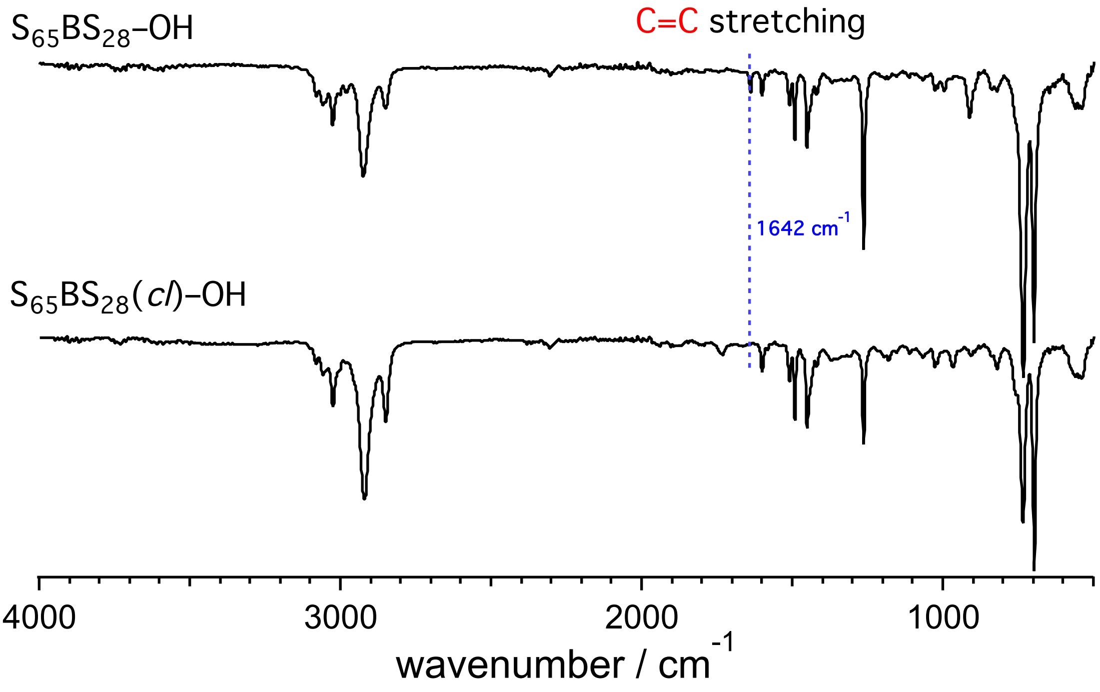

Figure S8. IR spectra of $S_{65}BS_{28}$–OH (upper) and $S_{65}BS_{28}$(*cl*)–OH (lower).

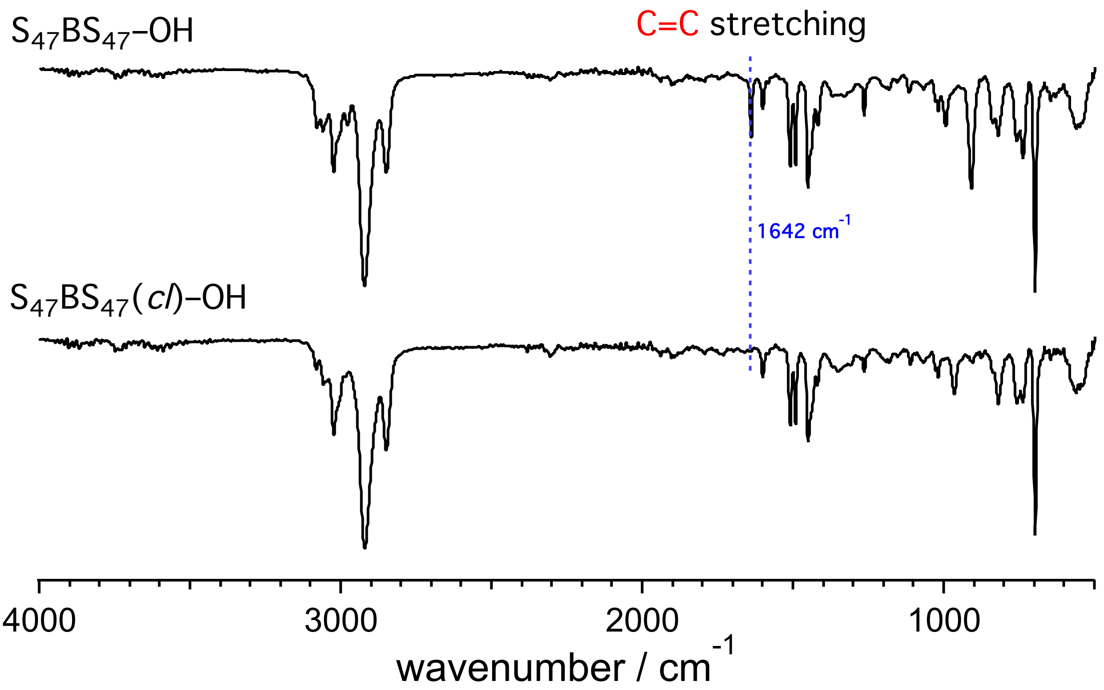

Figure S9. IR spectra of $S_{47}BS_{47}$–OH (upper) and $S_{47}BS_{47}$(*cl*)–OH (lower).

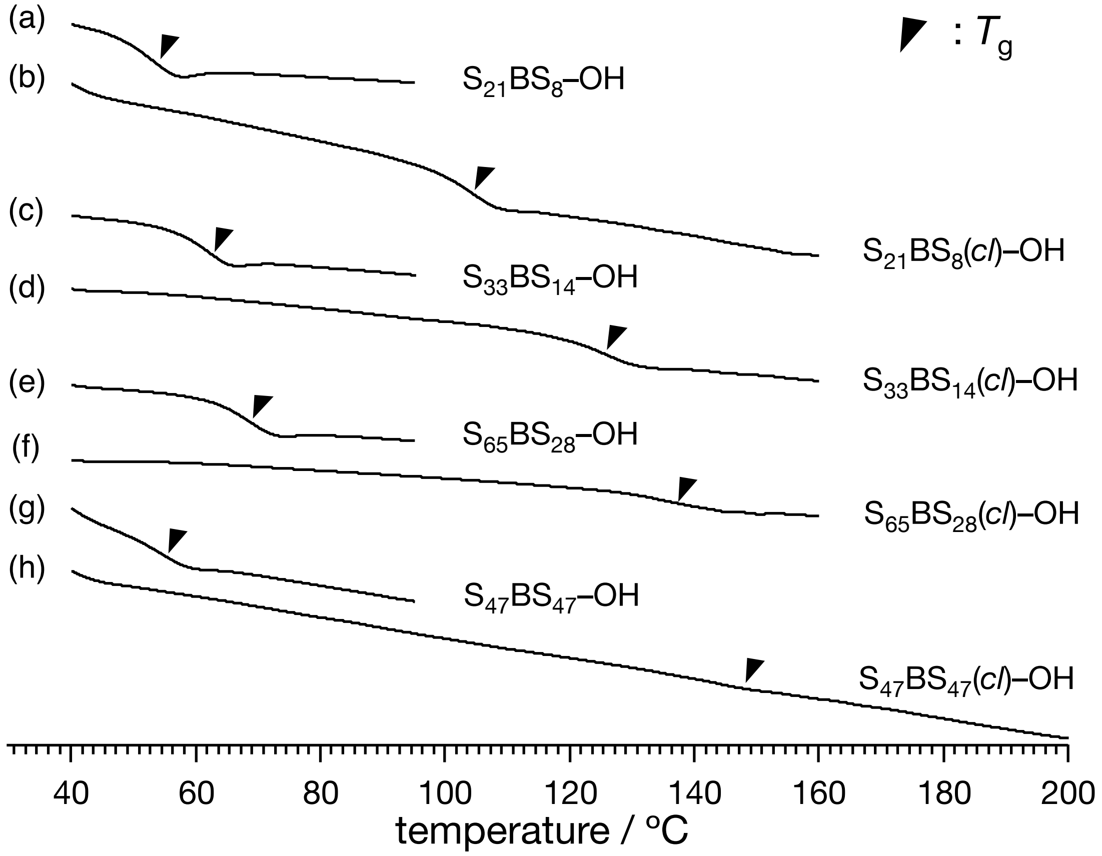

Figure S10. DSC curves during the 2nd heating process of (a) $S_{21}BS_8$–OH, (b) $S_{21}BS_8$(*cl*)–OH, (c) $S_{33}BS_{14}$–OH, (d) $S_{33}BS_{14}$(*cl*)–OH, (e) $S_{65}BS_{28}$–OH, (f) $S_{56}BS_{28}$(*cl*)–OH, (g) $S_{47}BS_{47}$–OH, and (h) $S_{47}BS_{47}$(*cl*)–OH.

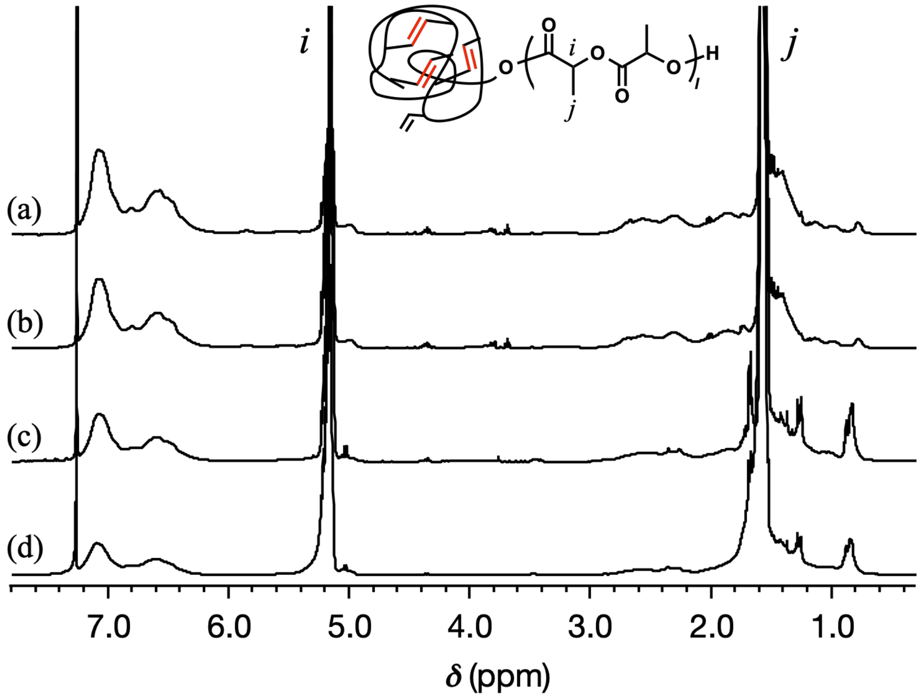

Figure S11. ^{1}H NMR spectra of (a) $\mathrm{S}_{21}\mathrm{BS}_{8}$(*cl*)–$\mathrm{LA}_{20}$, (b) $\mathrm{S}_{21}\mathrm{BS}_{8}$(*cl*)–$\mathrm{LA}_{45}$, (c) $\mathrm{S}_{21}\mathrm{BS}_{8}$(*cl*)–$\mathrm{LA}_{75}$, and (d) $\mathrm{S}_{21}\mathrm{BS}_{8}$(*cl*)–$\mathrm{LA}_{115}$ in CDCl_3 (400 MHz).

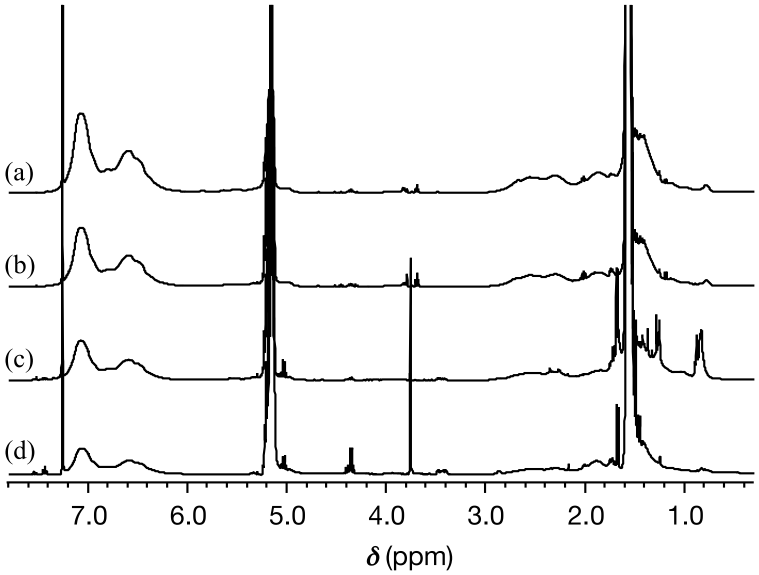

Figure S12. ^{1}H NMR spectra of (a) $\mathrm{S}_{33}\mathrm{BS}_{14}$(*cl*)–$\mathrm{LA}_{33}$, (b) $\mathrm{S}_{33}\mathrm{BS}_{14}$(*cl*)–$\mathrm{LA}_{72}$, (c) $\mathrm{S}_{33}\mathrm{BS}_{14}$(*cl*)–$\mathrm{LA}_{117}$, and (d) $\mathrm{S}_{33}\mathrm{BS}_{14}$(*cl*)–$\mathrm{LA}_{214}$ in CDCl_3 (400 MHz).

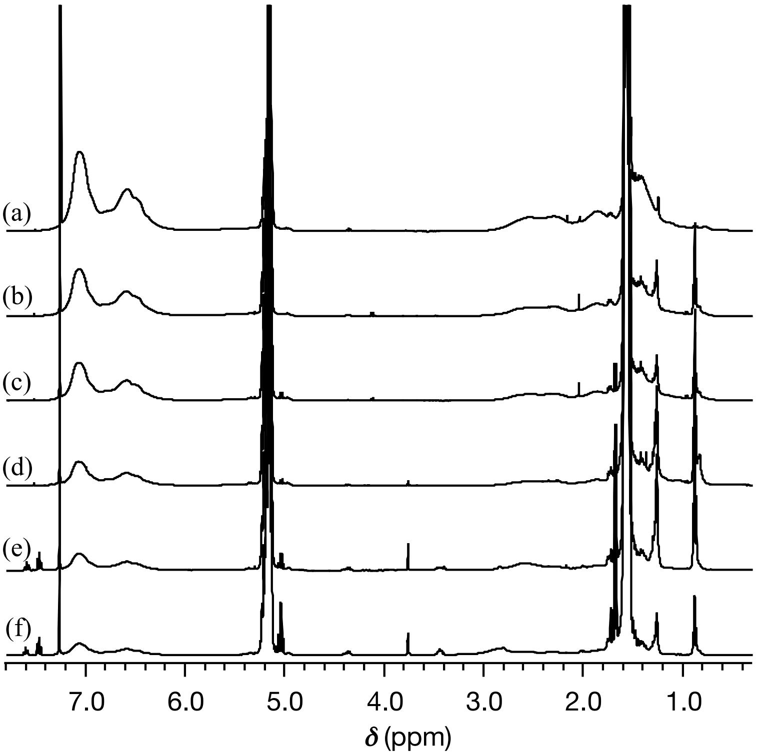

Figure S13. ^{1}H NMR spectra of (a) $S_{65}BS_{28}$(*cl*)–LA_{74}, (b) $S_{65}BS_{28}$(*cl*)–LA_{160}, (c) $S_{65}BS_{28}$(*cl*)–LA_{223}, (d) $S_{65}BS_{28}$(*cl*)–LA_{459}, (e) $S_{65}BS_{28}$(*cl*)–LA_{684}, and (f) $S_{65}BS_{28}$(*cl*)–LA_{923} in $CDCl_3$ (400 MHz).

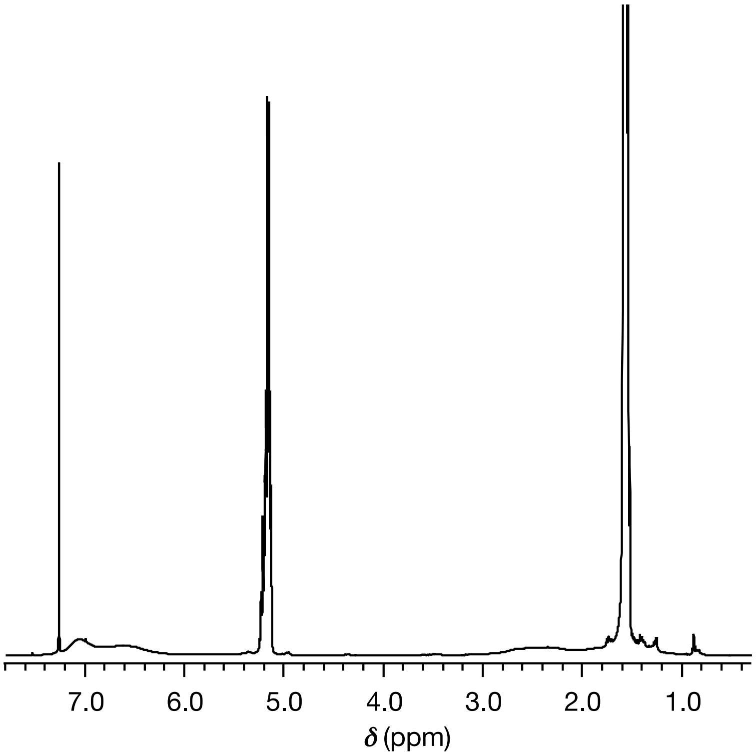

Figure S14. ^{1}H NMR spectra of $S_{47}BS_{47}$(*cl*)–LA_{484} in $CDCl_3$ (400 MHz).

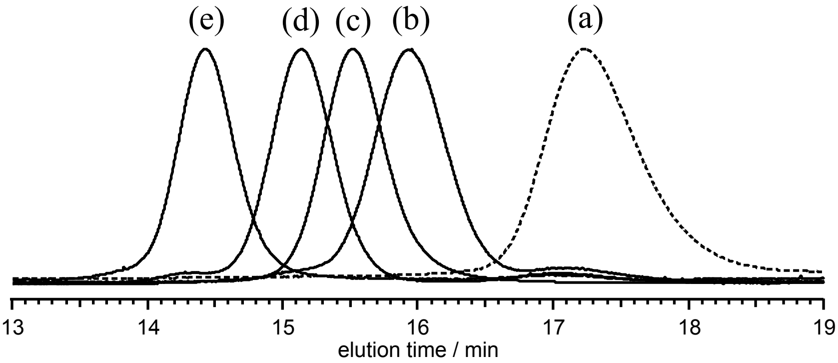

Figure S15. SEC traces of (a) $S_{21}BS_8$(*cl*)–OH macroinitiator, (b) $S_{21}BS_8$(*cl*)–LA_{20}, (c) $S_{21}BS_8$(*cl*)–LA_{45}, (d) $S_{21}BS_8$(*cl*)–LA_{75}, and (e) $S_{21}BS_8$(*cl*)–LA_{115} (eluent, THF; flow rate, 1.0 mL min^{-1}).

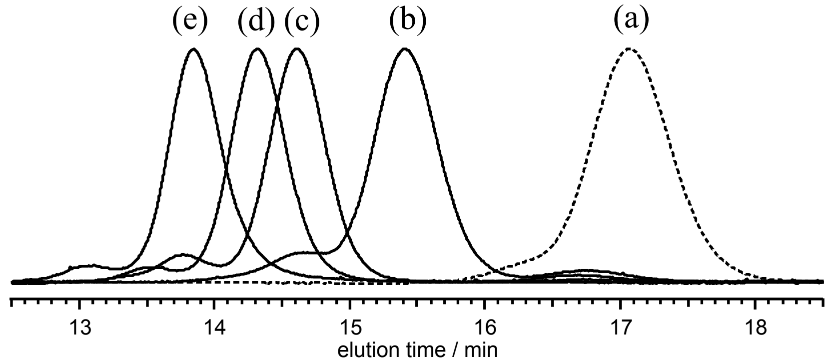

Figure S16. SEC traces of (a) $S_{33}BS_{14}$(*cl*)–OH macroinitiator, (b) $S_{33}BS_{14}$(*cl*)–LA_{33}, (c) $S_{33}BS_{14}$(*cl*)–LA_{72}, (d) $S_{33}BS_{14}$(*cl*)–LA_{117}, and (e) $S_{33}BS_{14}$(*cl*)–LA_{214} (eluent, THF; flow rate, 1.0 mL min^{-1}).

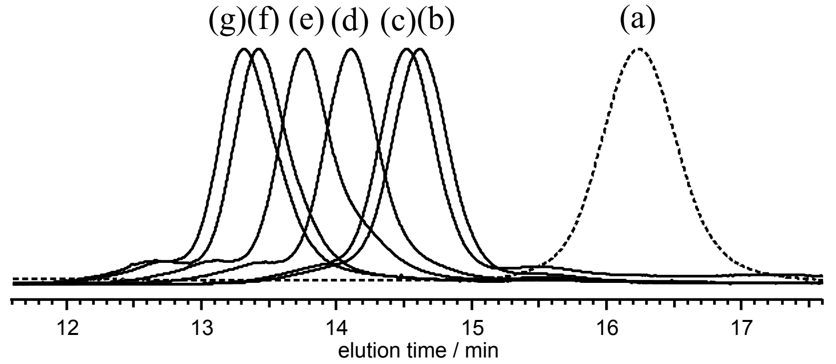

Figure S17. SEC traces of (a) $S_{65}BS_{28}$(*cl*)–OH macroinitiator, (b) $S_{65}BS_{28}$(*cl*)–LA_{74}, (c) $S_{65}BS_{28}$(*cl*)–LA_{160}, (d) $S_{65}BS_{28}$(*cl*)–LA_{223}, (e) $S_{65}BS_{28}$(*cl*)–LA_{459}, (f) $S_{65}BS_{28}$(*cl*)–LA_{684}, and (g) $S_{65}BS_{28}$(*cl*)–LA_{923} (eluent, THF; flow rate, 1.0 mL min^{-1}).

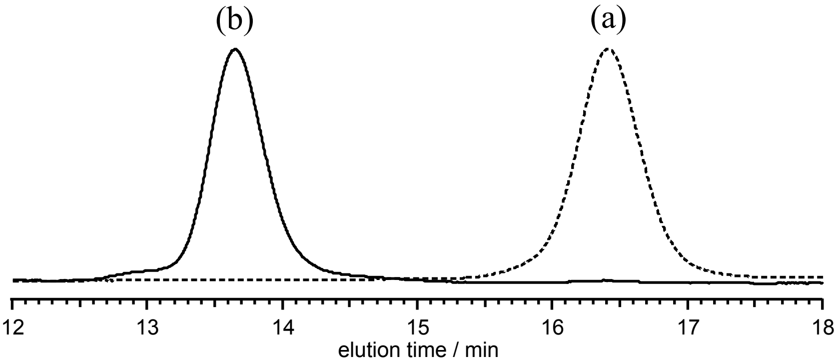

Figure S18. SEC traces of (a) $S_{47}BS_{47}$(*cl*)–OH macroinitiator and (b) $S_{47}BS_{47}$(*cl*)–LA_{484} (eluent, THF; flow rate, 1.0 mL min^{-1}).

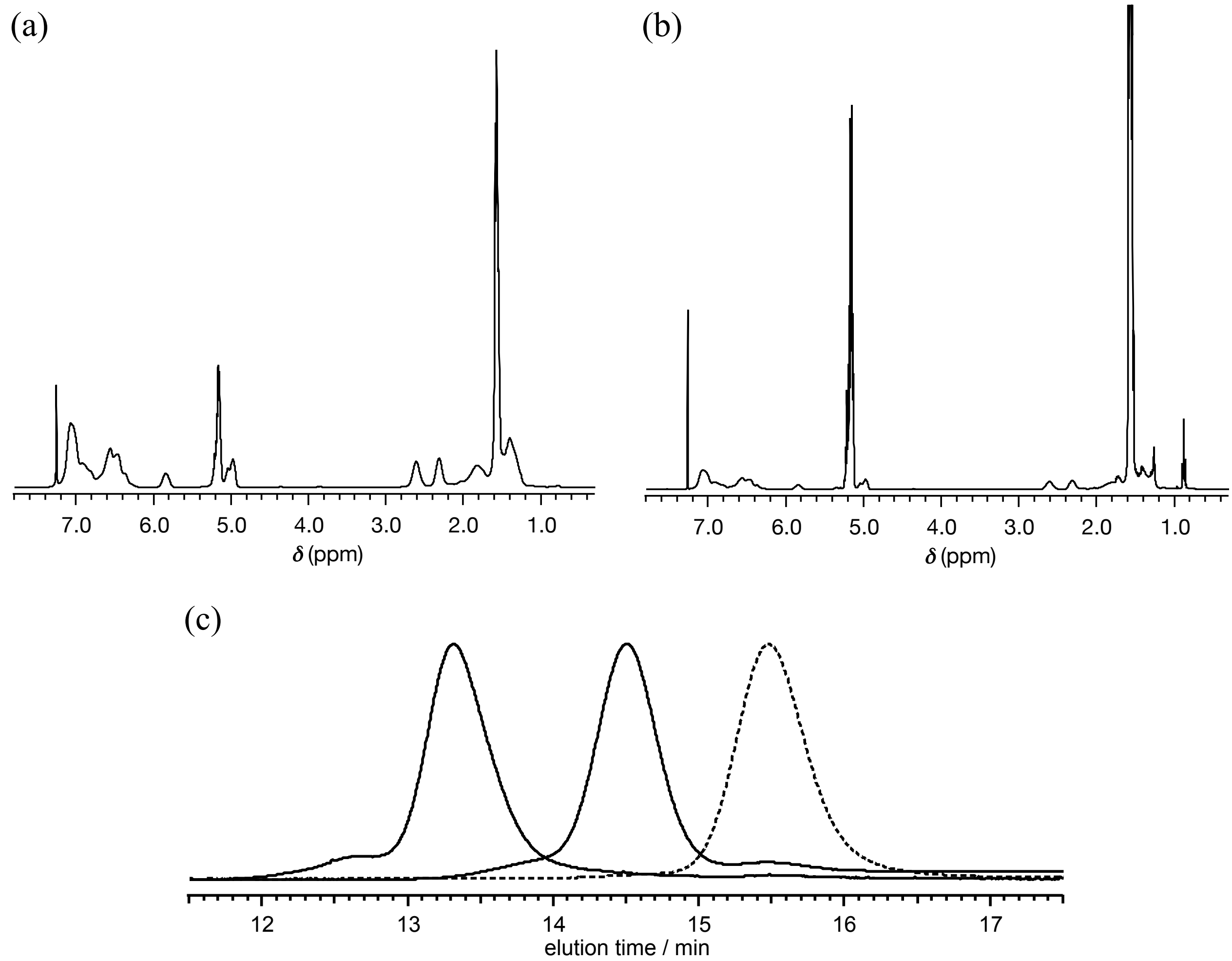

Figure S19. ^{1}H NMR spectrum of (a) $S_{65}BS_{28}$–LA_{67} and (b) $S_{65}BS_{28}$–LA_{466} in $CDCl_3$ (400 MHz). (c) SEC traces of $S_{65}BS_{28}$–OH macroinitiator (dashed line) and $S_{65}BS_{28}$–LA_{67} (right solid line) and $S_{65}BS_{28}$–LA_{466} (left solid line) (eluent, THF; flow rate, 1.0 mL min^{-1}).

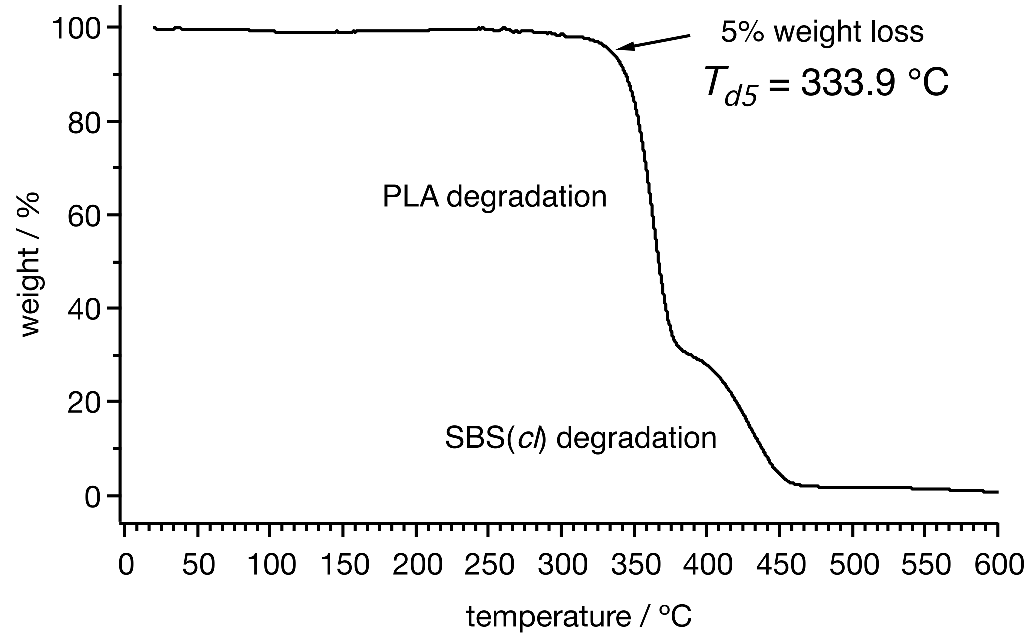

Figure S20. Thermogravimetric analysis profile of $S_{65}BS_{28}(cl)$–LA_{160}.

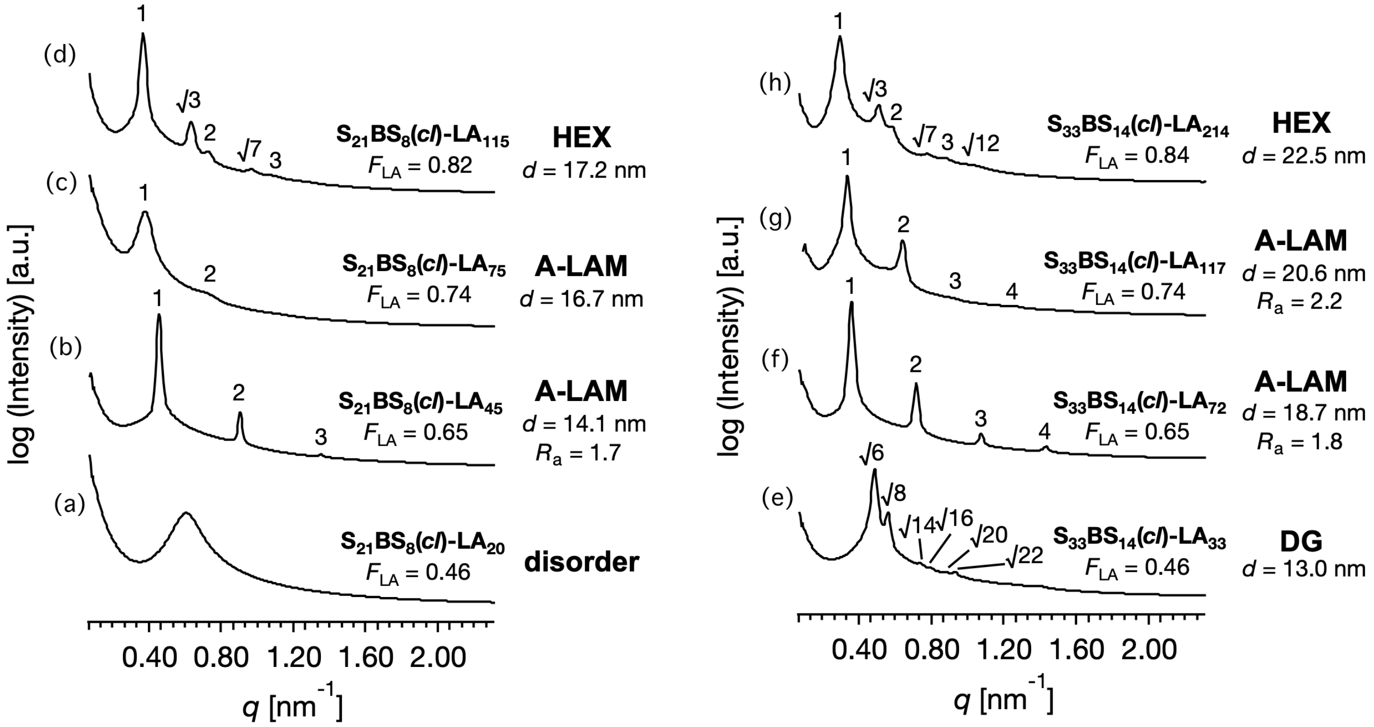

Figure S21. SAXS profiles of (a)-(d) $S_{21}BS_8(cl)$–LAs and (e)-(h) $S_{33}BS_{14}(cl)$–LAs.

Double gyroid (DG) morphology

One of the reasons for the formation of a DG morphology by $S_{33}BS_{14}(cl)$–LA_{33} (F_{LA} = 0.46) and $S_{65}BS_{28}(cl)$–LA_{74} (F_{LA} = 0.50) is quite clear: even though these BCPs possess symmetric block compositions, the bulkiness of the SBS(*cl*) block creates a driving force to bend the interface to the PLA domain side, resulting in slightly curved DG nanostructures. Importantly, the TEM images of the DG morphology of $S_{65}BS_{28}(cl)$–LA_{74} showed a dark SBS(*cl*) matrix with bright LA microdomains upon RuO_4 vapor staining,[4] which coincides with the above argument.

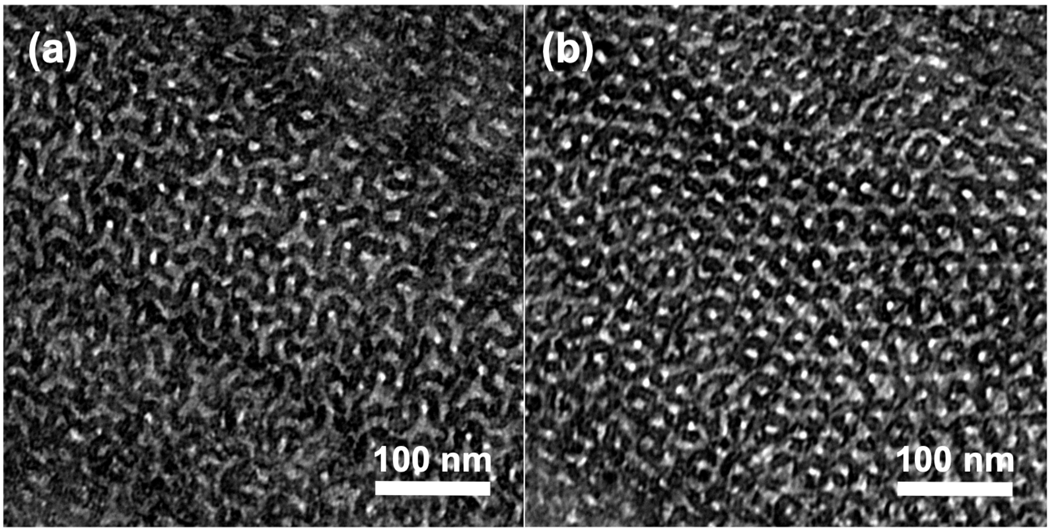

Figure S22. TEM images of the microtomed $S_{65}BS_{28}(cl)$–LA_{74} samples stained by RuO_4 vapor for 10 h. Images show the patterns of (a) (111) and (b) (110) planes of the DG morphology.

Correlation Function Analysis

The correlation function analysis was conducted by SasView 5.0. A real-space function, the so-called "1D electron density correlation function ($\Gamma(x)$)", can be obtained by the Fourier Transform (FT) of the reciprocal-space 1D SAXS profile. Under the assumption of a two-phase model consisting of the alternatively stacked layers, the widths of one domain (l_as) as well as domain-spacings (ds) in A-LAM structures were estimated by analyzing the obtained $\Gamma(x)$s using the method of Strobl and Schneider.[5,6]

The FT of the SAXS profiles of the samples were performed using the following equations:

$$\Gamma(x) = \frac{1}{Q*}\int_0^\infty I(q)q^2 cos(qx)dq$$

$$Q* = \int_0^\infty I(q)q^2 dq$$

wherein x, $I(q)$, and $Q*$ stand for the length scale in a real-space, scattering intensity, and scattering invariant, respectively. The l_as were assigned to the x value of intersection point of fitting and horizontal line drew from the first peak as seen in **Figure S23**. The width of the other domain (l_b) can be calculated according to $l_b = d - l_a$. Considering the facts that the width of SBS(cl) domain ($l_{SBS(cl)}$) should be smaller than that of LA one (l_{LA}) due to the weight fraction and l_b value is increased by increasing the molecular weight of PLA block, l_a and l_b must be $l_{SBS(cl)}$ and l_{LA}, respectively.

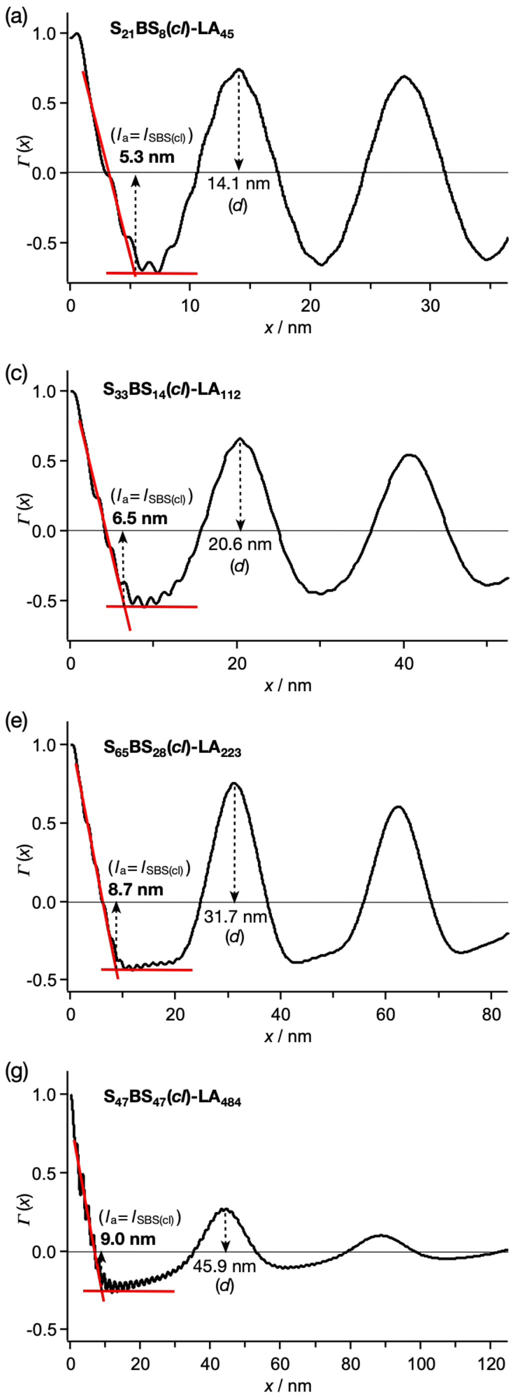

Figure S23. 1D electron density correlation functions obtained by the FT of the SAXS profiles of (a) S$_{21}$BS$_8$(*cl*)–LA$_{45}$, (b) S$_{33}$BS$_{14}$(*cl*)–LA$_{72}$, (c) S$_{33}$BS$_{14}$(*cl*)–LA$_{112}$, (d) S$_{65}$BS$_{28}$(*cl*)–LA$_{160}$, (e) S$_{65}$BS$_{28}$(*cl*)–LA$_{223}$, (f) S$_{65}$BS$_{28}$(*cl*)–LA$_{459}$, and (g) S$_{47}$BS$_{47}$(*cl*)–LA$_{484}$.

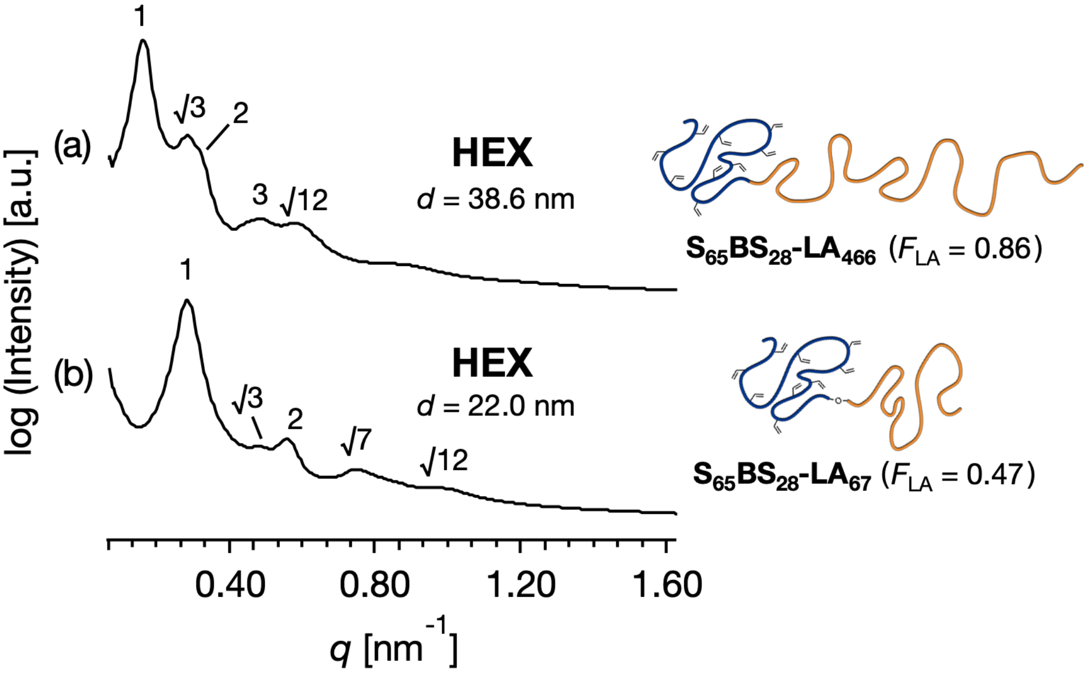

Figure S24. SAXS profiles of (a) $S_{65}BS_{28}$–LA_{466} and (b) $S_{65}BS_{28}$–LA_{67}.

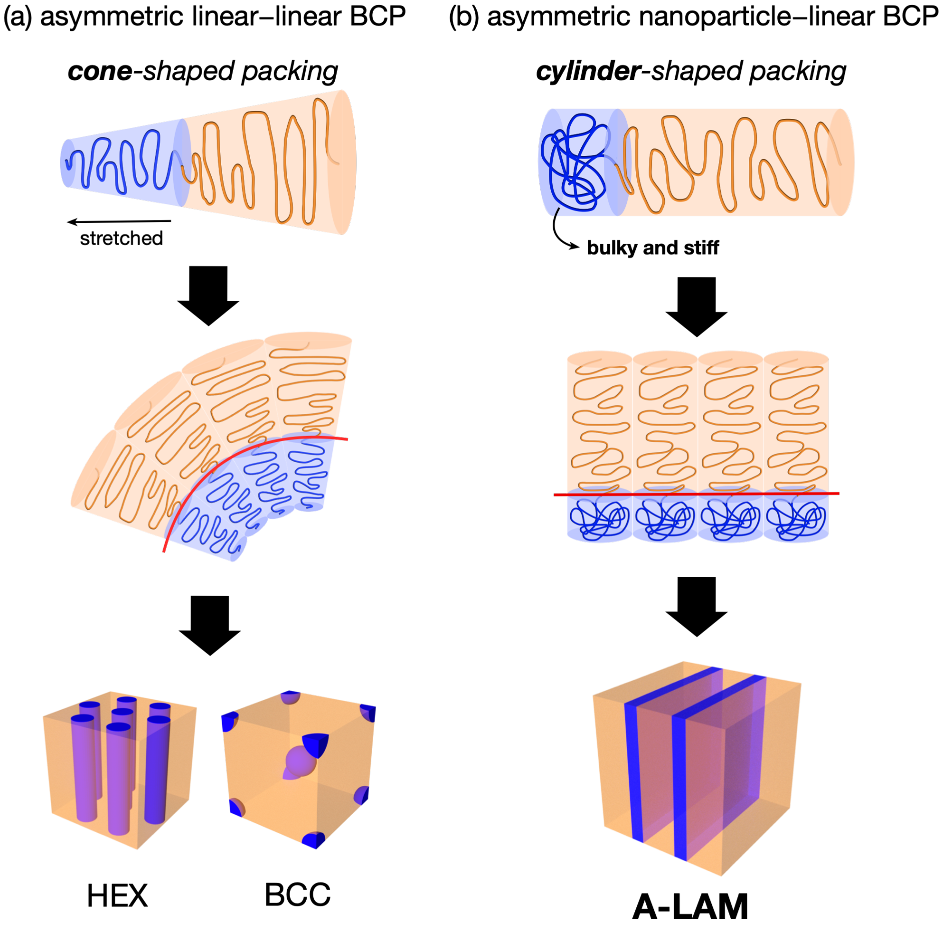

Figure S25. Schematic illustration of the packing models for the compositionally asymmetric (a) linear–linear and (b) nanoparticle–linear BCPs.

Guinier Analysis of SANS Data

The radius gyration (R_g) of the samples in the bulk was approximated by the Guinier analysis of the scattering data (**Figure S26a**) at the low q region according to the following equation (Guinier's low):

$$lnI(q) = lnI_0(q) - \frac{q^2 R_g{}^2}{3}$$

where $I_0(q)$ is the incident beam intensity. This approximation must satisfy the maximum qR_g of less than 1.33. Within this condition, the obtained scattering data can be plotted into a log$I(q)$ *vs.* q^2 curve (Guinier plots, **Figure S26b**), wherein the resulting slope of the curve, m, is used to give the approximate R_g values by the following equation:

$$R_g = \sqrt{-3m}$$

There are the steep increases in the intensity at low q region in the SANS profiles of $S_{65}BS_{28}$(*cl*)–OH and $S_{47}BS_{47}$(*cl*)–OH due to the parasitic scattering coming from the air gaps in the bulk samples. Therefore, the Guinier analysis was performed by discarding the data at very low-q region.[7]

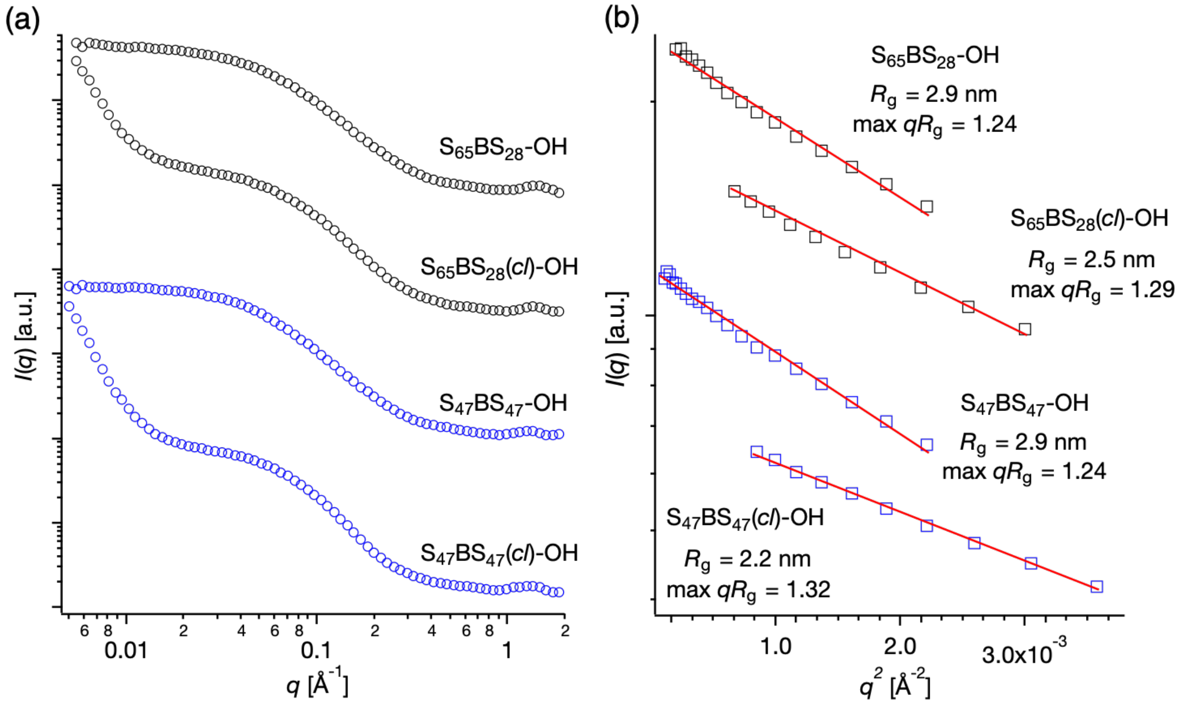

Figure S26. (a) SANS profiles and (b) Guinier plots of $S_{65}BS_{28}$–OH (black, upper), $S_{65}BS_{28}$(*cl*)–OH (black, lower), $S_{47}BS_{47}$–OH (blue, upper), and $S_{47}BS_{47}$(*cl*)–OH (blue, lower). The $I(q)$ data were vertically shifted by multiplying arbitrary constants.

The R_g of polystyrene in the theta condition (cyclohexane, 35 °C) is given by the following equation:

$$R_g[\mathrm{nm}] = 0.02675 \times M^{0.5040}[\mathrm{g\ mol^{-1}}]$$

where M is the molecular weight of the polystyrene. M is calculated to be 9,690 g mol^{-1} for the polystyrene with DP of 93, giving the R_g value of 2.7 nm. It is well known that the polymer chain dimensions in the bulk state is almost identical with that in the theta conditions.

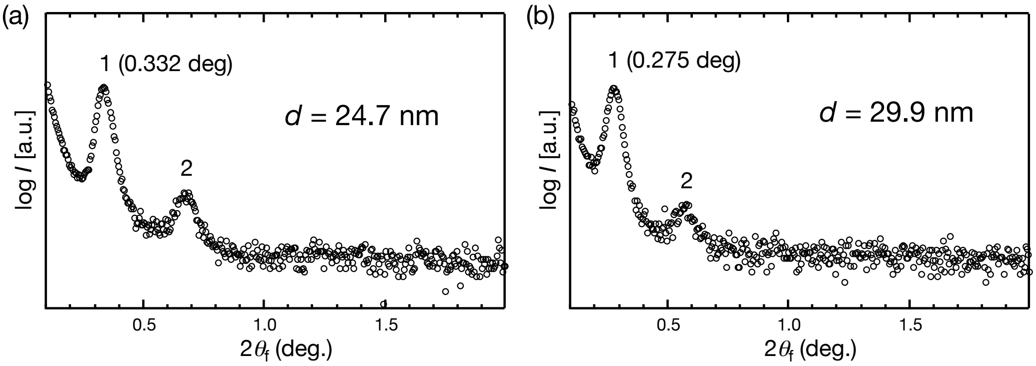

Figure S27. The in-plane scattering profiles extracted from the GISAXS images of (a) $S_{65}BS_{28}$(*cl*)–LA_{160} and (b) $S_{65}BS_{28}$(*cl*)–LA_{223} thin films along the $2\theta_f$ direction at α_f of 0.116° and 0.271°, respectively.

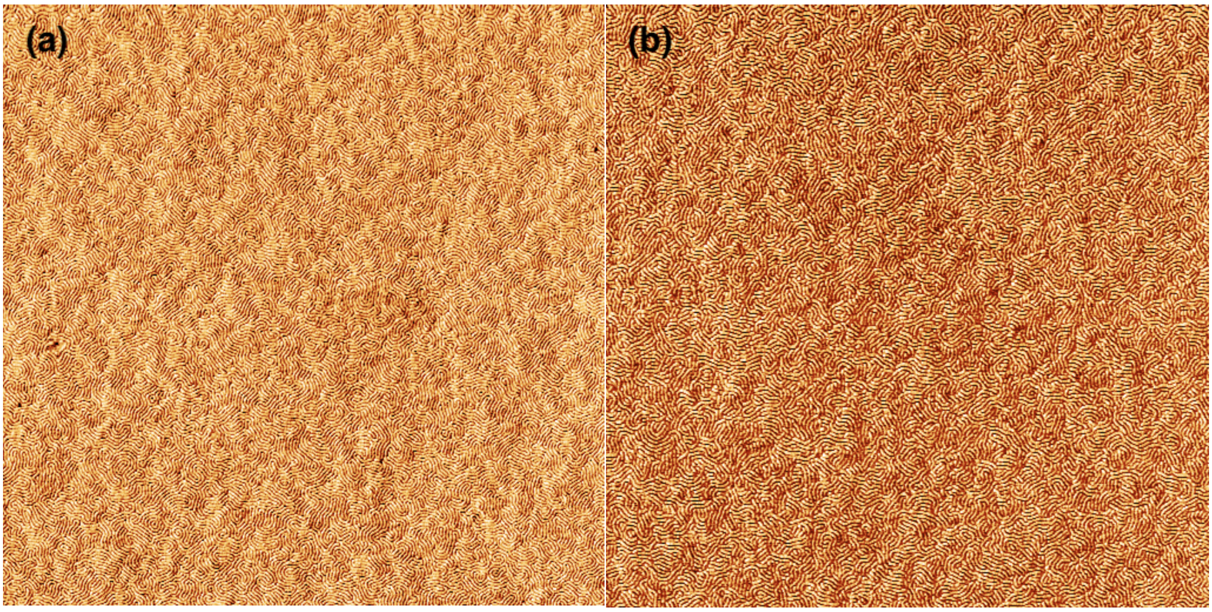

Figure S28. AFM phase images of (a) $S_{65}BS_{28}$(*cl*)–LA_{160} and (b) $S_{65}BS_{28}$(*cl*)–LA_{223} thin films. The images are 5 μm square.

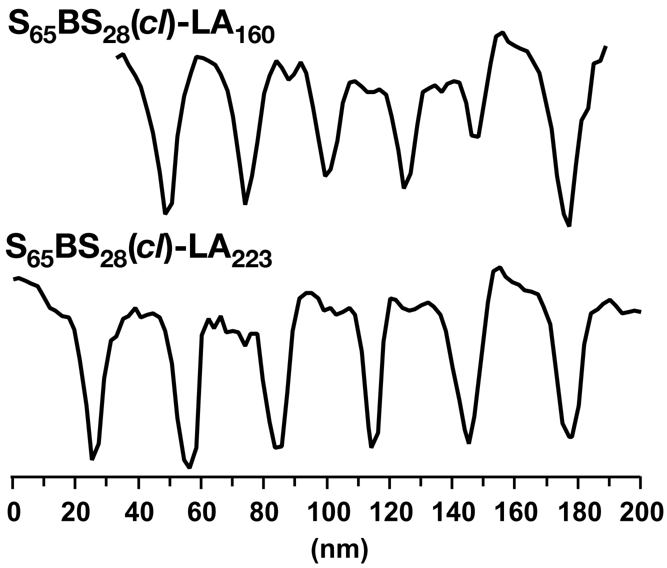

Figure S29. AFM cross-sectional profiles extracted along with the red lines in the phase images of $S_{65}BS_{28}(cl)$–LA_{160} (upper) and $S_{65}BS_{28}(cl)$–LA_{223} (lower) thin films (Figure 6).

S3. References

1. H. Zhang, E. Ruckenstein, *Macromolecules*, 1999, **32**, 5495.
2. J. Burdyńska, Y. Li, A. V. Aggarwal, S. Höger, S. S., Sheiko, K. Matyjaszewski, *J. Am. Chem. Soc.* 2014, **136**, 12762.
3. S. Takata, J. Suzuki, T. Shinohara, T. Oku, T. Tominaga, K. Ohishi, H. Iwase, T. Nakatani, Y. Inamura, T. Ito, *et al.*, *JPS Conf. Proc.* 2015, **8***,* 036020.
4. a) H. Wang, L. Yu, X. Wang, R. Ho, *Macromolecules* 2014**, 47,** 7993.; b) N. Y. Ahn, M. Seo, *RSC Adv.* 2016, **6**, 47715.
5. a) G. R. Strobl, M. Schneider, *J. Polym. Sci.* 1980**, 18,** 1343.; b) Gert R. Strobl, *The Phisics of Polymers: Concepts for Understanding Their Structures and Behavior*, Springer Science & Business Media, 2007
6. K. S. Anderson, M. A. Hillmyer, *Macromolecules* 2004, **37**, 1857.